PHILOSOPHICAL TRANSACTIONS OF THE ROYAL SOCIETY A MATHEMATICAL, PHYSICAL & ENGINEERING SCIENCES

A Non-Gaussian Model for Random Surfaces

R. J. Adler and D. Firman

Phil. Trans. R. Soc. Lond. A 1981 **303**, 433-462
doi: 10.1098/rsta.1981.0214

Phil. Trans. R. Soc. Lond. A **303**, 433–462 (1981) [433]
Printed in Great Britain

A NON-GAUSSIAN MODEL FOR RANDOM SURFACES

BY R. J. ADLER† AND D. FIRMAN‡
† *Faculty of Industrial Engineering and Management, Technion – Israel Institute of Technology, Haifa, Israel*
‡ *Department of Statistics, University of New South Wales, Kensington, N.S.W., Australia*

(*Communicated by D. G. Kendall, F.R.S. – Received* 23 *October* 1980 – *Revised* 16 *February* 1981)

CONTENTS

The central concern of this paper is to develop for rough (two-dimensional, metallic) surfaces a model other than the Gaussian one usually used. An analysis, via the notion of 'upcrossing characteristics', of some new data on abraded stainless steel, as well as a new look at some old data, indicates the need for such a model. The model adopted is of a form that gives χ^2-type marginal height distributions for the surface.

After the new model has been introduced and motivated, its properties are investigated in some detail. In particular, the properties of the surface and its profiles at local

maxima are studied by examining, for example, the height distribution and the surface curvature at such points. Phenomena are observed that are notably, qualitatively, different to what happens in the Gaussian model.

Although the model introduced here is motivated by problems in the study of metallic surfaces, we believe it to be useful in other areas. Consequently, those sections of the paper that investigate the properties of the model are written so as to be independent of the original motivation. The paper also reintroduces, in an applied setting, the idea of examining surfaces via their upcrossing characteristics.

1. Introduction

It is a well established fact that all surfaces used in engineering practice are rough when judged by the standards of microscopic measurement. Moreover, this roughness plays an essential role in determining macroscopic phenomena such as the friction, electric contact, and adhesion between two macroscopically smooth surfaces. Because of the impossibility of specifying the exact form of any given surface, mathematical models of random surfaces have been used to considerable advantage over the last fifteen years to derive the macroscopic properties of a surface from an essentially microscopic description of its roughness. The first of these random models was proposed by Greenwood & Williamson (1966). The so-called *three-point model*, which we shall discuss below, was later developed by Whitehouse & Archard (1970), and a theory of contact was derived from this model by Onions & Archard (1973). A recent review of the problems of rough surfaces and applications of random models to these problems is given by Archard *et al.* (1975).

A more complete, and in many ways more rigorous, approach to the characterization of rough surfaces has been made by Nayak (1971, 1973*a*, *b*), building on the models developed by Longuet-Higgins (1957*a*, *b*) to describe ocean surfaces. Nayak's model has found numerous applications, including a random rough surface model for adhesion by Bush *et al.* (1976), which develops further a model studied by Fuller & Tabor (1975), Johnson *et al.* (1971) and Johnson (1975).

One aspect that all of the above models have in common is the underlying assumption that the random surface has a *Gaussian*, or *normal*, distribution. Although attempts to justify this assumption are often made by appealing to the apparent normality of actual surfaces, the main justification has lain in the fact that only Gaussian models have appeared to be analytically tractable. This, of course, is due to the eminently simple and elegant form of the multivariate normal probability density, which makes possible analytic manipulations that seem almost impossible to do for other distributions. Nevertheless, it is the contention of this paper that neither of the above reasons is sufficient to justify limiting consideration to only the Gaussian model. In § 3 we present some new experimental data, and re-examine some old, that indicate that the assumption of normality is often contra-indicated. In the subsequent sections we undertake an analytic examination of a non-Gaussian model suggested by the data. The model itself will be introduced in § 2.

Before we begin our study, however, it is probably worth while to make two comments about the scope of this paper. The first is to note that, while the principal motivation for introducing the model we shall consider comes from the field of surface roughness, there is good reason to expect that it may also be useful in other disciplines where random surfaces have found acceptance as mathematical models. In particular, it would seem to be readily applicable to the modelling of wind strength, where similar one-dimensional (or profile) models have already proven useful (see, for example, Davenport 1967, Hasofer 1972*a*, *b*.) Consequently, the paper has been written

in such a way that the terminology used and approach taken are those of general statistical analysis rather than those specific to the discipline of rough surfaces.

Secondly, we must, in all honesty, note that having developed and investigated our model for rough surfaces, we do not apply it to specific problems, such as wear and adhesion. We intend to tackle some of these problems in a separate work.

2. The χ_n^2-model

We commence by describing the Gaussian model. We shall use upper case italic letters for random variables and surfaces, (s, t), $-\infty \leqslant s, t \leqslant \infty$, to denote a point on the plane, and Greek letters for parameters relating to the distributions of random objects. We say that $X(s, t)$ is a *Gaussian*, or *normal*, random surface if the collection of random variables $\{X(s_1, t_1), \ldots, X(s_k, t_k)\}$ possesses a multivariate normal distribution for every collection of points $(s_1, t_1), \ldots, (s_k, t_k)$. Let us now make the assumption that the mean of $X(s, t)$ is zero, and, furthermore, that X is a *homogeneous* surface. That is, the statistical properties of the variables $\{X(s_1+a, t_1+b), \ldots, X(s_k+a, t_k+b)\}$ are independent of a and b. Then the distribution of the surface X is completely specified by its *covariance function*, $R_X(s, t)$, which can be defined either by

$$R_X(s,t) = \mathscr{E}[X(0,0)\, X(s,t)], \tag{2.1}$$

where $\mathscr{E}$ denotes statistical expectation, or by

$$R_X(s,t) = \lim_{T\to\infty} \frac{1}{4T^2} \int_{-T}^{T}\int_{-T}^{T} X(0,0)\, X(s,t)\, \mathrm{d}s\, \mathrm{d}t. \tag{2.2}$$

(Strictly, (2.1) and (2.2) are only equivalent when X is *ergodic*. For details see, for example, Adler (1981).

Several useful statistical parameters are easily obtained from $R_X(s, t)$. The standard deviation, σ_x, of the distribution of $X(s, t)$ is given by $\sigma_x^2 = R_X(0, 0)$. Writing down the Fourier representation

$$R_X(s,t) = \int_{-\infty}^{\infty}\int_{-\infty}^{\infty} \exp\left[\mathrm{i}(sx+ty)\right] f_X(x,y)\, \mathrm{d}x\, \mathrm{d}y \tag{2.3}$$

of R_X, yields the spectral density $f_X(x, y)$ of $X(s, t)$ that can be used to describe its decomposition into harmonic, or wavefunction, components. Using the spectral density we can define sets of second- and fourth-order spectral moments, λ_{ij} and ν_{ij} respectively, that will be extremely important in the forthcoming analysis:

$$\left.\begin{aligned} \lambda_{ij} &= \int_{-\infty}^{\infty}\int_{-\infty}^{\infty} s^i t^j f_X(s,t)\, \mathrm{d}s\, \mathrm{d}t, \quad i+j=2, \\ \nu_{ij} &= \int_{-\infty}^{\infty}\int_{-\infty}^{\infty} s^i t^j f_X(s,t)\, \mathrm{d}s\, \mathrm{d}t, \quad i+j=4. \end{aligned}\right\} \tag{2.4}$$

With application of the representation (2.3) it is straightforward to check that the $2k$th-order spectral moments are obtainable from the $2k$th-order derivatives of $R_X(s, t)$ at $(0, 0)$. Thus

$$\lambda_{ij} = \left.\frac{-\partial^2 R(s,t)}{\partial s^i t^j}\right|_{s=t=0}, \quad \nu_{ij} = \left.\frac{\partial^4 R(s,t)}{\partial s^i t^j}\right|_{s=t=0}. \tag{2.5}$$

Furthermore, (2.1) easily yields that $2k$th-order spectral moments are the variances of the kth-order partial derivatives of the surface $X(s, t)$, and that the covariance functions of these derivatives

are merely the appropriate $2k$th-order partial derivatives of $R_X(s,t)$. Indeed, we also have the important general formula

$$\mathscr{E}\left[\frac{\partial^{\alpha+\beta}X(s,t)}{\partial s^\alpha\,\partial t^\beta}\,\frac{\partial^{\gamma+\delta}X(s,t)}{\partial s^\gamma\,\partial t^\delta}\right] = \left.\frac{\partial^{\alpha+\beta+\gamma+\delta}R_X(s,t)}{\partial s^{\alpha+\gamma}\,\partial t^{\beta+\delta}}\right|_{s=t=0}$$
$$= (-1)^{\alpha+\beta}i^{\alpha+\beta+\gamma+\delta}\int_{-\infty}^{\infty}\int_{-\infty}^{\infty} s^{\alpha+\gamma}t^{\beta+\delta}f_X(s,t)\,\mathrm{d}s\,\mathrm{d}t. \qquad (2.6)$$

Relations (2.4)–(2.6) are extremely important in the study of Gaussian surfaces, for implicit in them is the fact that the multivariate density of the surface $X(s,t)$ and any of its partial derivatives is multivariate, normal, and dependent only on its spectral moments. Indeed, it is this latter fact that makes Gaussian surfaces so readily amenable to statistical investigation.

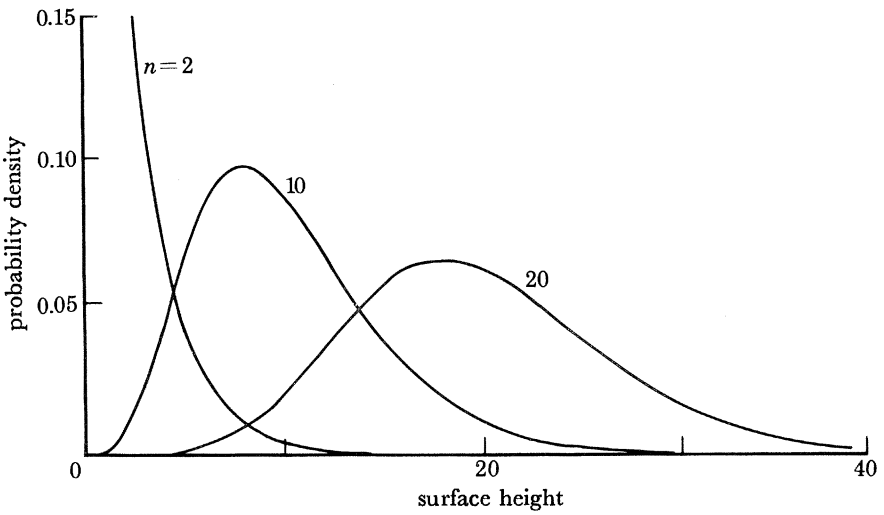

FIGURE 1. χ^2_n probability densities.

Noting all these facts, we can now proceed to build a different random surface which, while exhibiting qualitatively different behaviour, possesses much of the mathematical simplicity of the Gaussian model. To do this we take n, $n \geqslant 1$, independent Gaussian surfaces $X_1(s,t), \ldots, X_n(s,t)$ and define the *χ^2_n-surface*

$$Y(s,t) = [X_1(s,t)]^2 + \ldots + [X_n(s,t)]^2. \qquad (2.7)$$

It is straightforward to check that the probability density for $Y(s,t)$ is that of a scaled χ^2_n random variable with n degrees of freedom, so that it is of the form

$$p(y) = [\sigma_x^n\, 2^{\frac{1}{2}n}\, \Gamma(\tfrac{1}{2}n)]^{-1}\, y^{\frac{1}{2}(n-2)} \exp(-\tfrac{1}{2}y/\sigma_x^2), \quad y \geqslant 0. \qquad (2.8)$$

Graphs of this density for various values of n, and $\sigma_x^2 = 1$, are given in figure 1. It is clear from these graphs that the distribution of $Y(s,t)$ is skewed to the right, the amount of skewness being inversely proportional to the parameter n. In the extreme cases of $n = 1$ and $n = 2$ the density descends monotonically from $y = 0$. The case $n = 2$ corresponds to $Y(s,t)$ having a *negative exponential* distribution and, as is well known in wind modelling, to $Y(s,t)^{\frac{1}{2}}$ having a *Raleigh* distribution.

Later we shall see that rough surface data often exhibit skewness in the opposite direction to that displayed in figure 1. We shall overcome this difficulty by working ultimately with a model of the form

$$Z(s,t) = M - Y(s,t) \tag{2.9}$$

where M is a predetermined constant. We shall call a random surface of this form an *M-inverted χ^2_n-surface*. For the moment, however, we shall deal only with simple χ^2_n-surfaces.

An immediate consequence of the definitions (2.7) and (2.1) is that the mean of $Y(s,t)$ is $n\sigma_x^2$, and its standard deviation is $(2n)^{\frac{1}{2}}\sigma_x^2$. Similarly, its covariance function is given by

$$\begin{aligned} R_Y(s,t) &= \mathscr{E}\{[Y(0,0) - n\sigma_x^2][Y(s,t) - n\sigma_x^2]\} \\ &= 2nR_X^2(s,t), \end{aligned} \tag{2.10}$$

where the second equality follows by applying standard results on the moments of normal variables.

The importance of (2.10) lies in the fact that once $R_Y(s,t)$ and n are specified so is $R_X(s,t)$. But since R_X determines the distribution of the random surfaces $X_j(s,t)$, and these determine $Y(s,t)$, it follows that the distribution of $Y(s,t)$ is completely determined once n and $R_Y(s,t)$ are given, and this determination incorporates, via the $X_j(s,t)$, a certain amount of 'normality'. It is this fact that makes the statistical analysis of χ^2_n-surfaces mathematically tractable. We shall commence this analysis after providing some justification for the application of this model to rough surfaces.

3. Justification of the χ^2_n-surface

(a) *Experimental data: new and old*

The data that actually motivated the present study originally came to our attention through the work of Silverman (1980), where they were used to provide an example of a form of non-parametric density estimation. They were collected by Dr Adrian Bowyer of the University of Bath, who studied them in Bowyer & Cameron (1977) and Bowyer (1980), and who very kindly made them available to us. The data represent the heights, measured in micrometres, of a specimen of stainless steel, with zero height corresponding to a least-squares-fit, mean plane through the data. The observations were taken on a 50×300 square grid, the rows and columns of the grid being 10 μm apart. Thus the specimen actually measured 0.5 mm × 3 mm. The data were gathered by using a Talysurf machine linked to an analogue-to-digital converter and a data logger. Before the surface was mapped it had been ground (in a direction parallel to the 3 mm tracks) and abraded with 400 grit emery paper. Figure 2 depicts the histogram of the 15 000 data points. Drawn on the same figure is a histogram of a normal distribution with the same mean and variance as that of the data.

It is immediately apparent from figure 2 that the histogram of surface heights shows a marked skewness to the left, indicating that the distribution of, say, the heights of the local maxima should also show a marked skewness to the left, compared with what one would expect if the surface distribution were Gaussian. (The histogram skewness is perhaps even more clearly depicted in figure 9 of Silverman (1980), where a smoothed version of it is given.) The skewness, however, is most clearly identified in figure 3, where the proportion of the surface lying below a specified height is plotted on normal probability paper, which has a distorted vertical scale so that a Gaussian distribution of heights will appear as a straight line. The graph here is, however,

certainly not straight, but shows the characteristic convexity indicative of left-skewness in the original data.

To our surprise, given the general acceptance the Gaussian model has gained in surface science, the skewness exhibited by Bowyer's data turns out to be not at all uncommon. For example, in the paper that introduced the Gaussian model, Greenwood & Williamson (1966) present normal probability plots of two sets of data. One yields a graph that could be reasonably accepted as a straight line, but the second, reproduced here as figure 4, exhibits precisely the same type of deviation from normality as that presented by Bowyer's data.

In relation to this data, Greenwood & Williamson make the following comment: 'Although the surface is at first sight highly non-Gaussian, in fact nearly 90 % of the surface is approximately

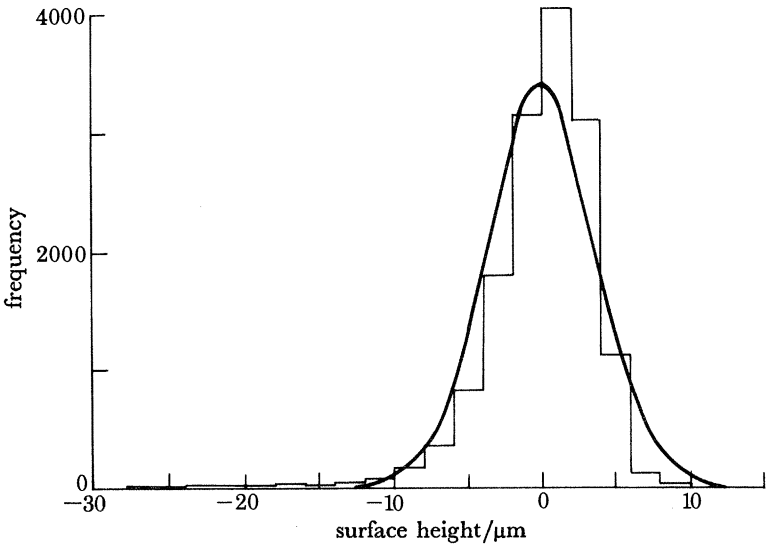

FIGURE 2. Histogram of surface heights for abraded stainless steel. The continuous curve is the Gaussian with the same mean and variance.

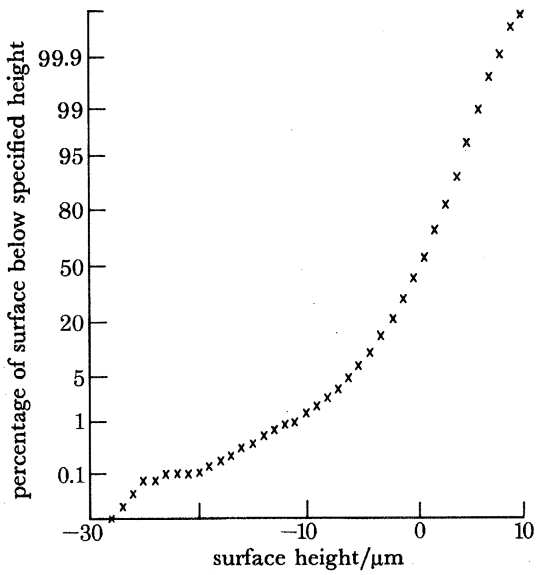

FIGURE 3. Cumulative height distribution of abraded stainless steel specimen whose histogram is given in figure 2.

Gaussian; the surface . . . would behave in contact as if Gaussian . . .'. We find it difficult to accept this claim for two reasons. First, it is a well established statistical fact that almost any unimodal distribution will look 'approximately Gaussian' over a considerable part of its range when mapped on normal probability paper. The important phenomenon is not how much apparent agreement there is, but rather the extent of the curvature in the graph. This is considerable in figure 4. Secondly, in surface science, the distribution of asperities is the determining factor in describing the macroscopic properties of the model. Since it is reasonable to expect that this distribution will in turn be primarily determined by the right-hand tail of the surface height distribution, it is imperative that the model fits well at this end, regardless of its fit to the main bulk of the distribution.

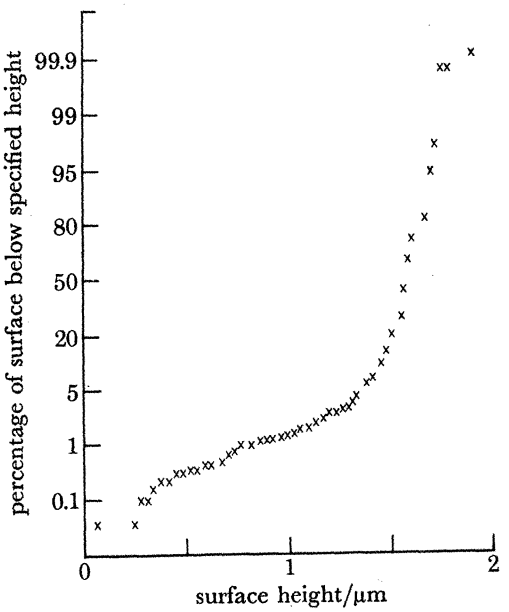

FIGURE 4. Cumulative height distribution of mild steel specimen of Greenwood & Williamson (1966). Note the similarity to the stainless steel specimen of figure 3.

We could continue in this fashion for some time, presenting yet more data sets exhibiting skewness. However, we shall let these two suffice to demonstrate our contention regarding the non-normality of many actual surfaces, and now proceed to see if a simple-minded approach can be developed to overcome this problem.

(*b*) *Transforming to normality*

The most obvious response to a Gaussian model and data of the form shown in figures 3 and 4 is to transform the data to normality. In one respect, this is easily done, and figure 5 shows normal probability plots of the two transformations

$$Y_1(s,t) = \ln[10 - Y(s,t)], \tag{3.1}$$

$$Y_2(s,t) = \{\ln[10 - Y(s,t)]\}^{\frac{1}{2}}. \tag{3.2}$$

Both of these transformations produce data that look far more normal than do the original data. It is unfortunate, however, that merely transforming a non-Gaussian random surface in such

a way that its height distribution becomes normal does not suffice to guarantee that the surface is actually a Gaussian surface. For this stronger condition to be satisfied it is necessary that all collections of random variables $\{Y_i(s_1, t_1), \ldots, Y_i(s_k, t_k)\}$ have an appropriate multivariate normal distribution.) To determine whether or not the transformations (3.1) and (3.2) actually yield Gaussian surfaces it is necessary to concentrate on some aspect of the surface that reflects its multivariate distribution. The aspect upon which we shall concentrate is a measure of the *level crossing behaviour*, as determined via a concept known as the *upcrossing characteristic*, which we shall now develop.

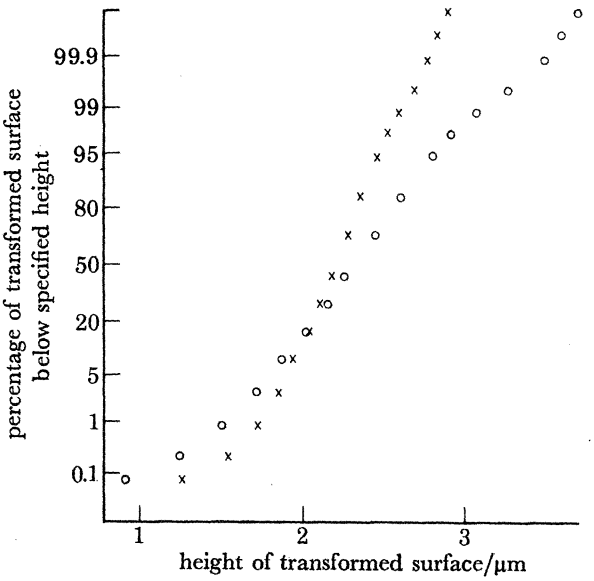

FIGURE 5. Cumulative height distribution of stainless steel specimen after height transformation ×, transformation (3.1); ○, transformation (3.2).

(c) *Upcrossing characteristics*

In dealing with stochastic processes $X(t)$ defined on the real line, one way to examine the correctness of an assumed model that is particularly relevant to the problems of central concern here is to investigate its level crossing behaviour. For example, if $X(t)$ is a zero-mean, homogeneous, Gaussian stochastic process with

$$\sigma^2 = \mathscr{E}[X^2(t)], \quad \lambda_2 = \mathscr{E}[(\mathrm{d}X(t)/\mathrm{d}t)^2], \tag{3.3}$$

and $N_X(u, T)$ denotes the number of upcrossings of the level u by $X(t)$, $0 \leqslant t \leqslant T$, then

$$\mathscr{E}[N_X(u, T)] = (T\lambda_2^{\frac{1}{2}}/2\pi\sigma) \exp(-u^2/2\sigma^2). \tag{3.4}$$

(see, for example, Cramér & Leadbetter 1967). However, if $Y(t) = X_1^2(t) + \ldots + X_n^2(t)$ is a χ_n^2-process, and each of the $X_i(t)$ has variance σ^2 and second spectral moment λ_2 as in (3.3), then the expected upcrossing rate for $Y(t)$ is different to that given by (3.4). In fact

$$\mathscr{E}[N_Y(u, T)] = \frac{T}{\Gamma(\frac{1}{2}n)\sigma}\left(\frac{\lambda_2}{\pi}\right)^{\frac{1}{2}}\left(\frac{u}{2\sigma^2}\right)^{\frac{1}{2}(n-1)} \exp(-u/2\sigma^2) \tag{3.5}$$

(see, for example, Hasofer 1974, Sharpe 1978). These two upcrossing rates are markedly different, and so comparing the observed up-crossing rate of a particular set of data with the expected rate often gives a good indication of which model is appropriate.

While it is possible to apply the results for stochastic processes in univariate time to random surfaces by using profile data, it is more efficient to use the full two-dimensional nature of the surface. To do this it is necessary to generalize the notion of upcrossings from processes to surfaces, a generalization most effectively achieved through the *upcrossing characteristic*, as introduced in Adler & Hasofer (1976) and described in considerable detail in Adler (1981).

To define this concept, let $S = [0, a] \times [0, b]$ be a rectangular region in the plane, and let $A_u(X, S)$ denote the *excursion set* of $X(s, t)$ above the level u, over the rectangle S. Formally

$$A_u(X, S) = \{(s, t) \in S : X(s, t) \geqslant u\}.$$

The upcrossing characteristic $\varphi(A_u)$ of the excursion set is then defined as

$$\varphi[A_u(X, S)] = \sum_x [N_u(x) - N_u(x^-)], \tag{3.6}$$

where, if we denote by E_x the horizontal line with points having coordinates (s, x) for $0 \leqslant s \leqslant a$,

$$\left.\begin{aligned} N_u(x) &= \begin{cases} \text{number of disjoint closed intervals in } A_u \cap E_x \text{ if } X(0, x) < u, \\ \text{the above number minus one if } X(0, x) \geqslant u, \end{cases} \\ N_u(x^-) &= \lim_{y \to x} N_u(y) \quad (y < x). \end{aligned}\right\} \tag{3.7}$$

The summation in (3.6) is over all $x \in (0, a]$ for which the summand is non-zero. There is only a finite number of such values of x.

Two examples of how to compute φ are given in figure 6, in which the enclosed areas represent excursion sets A_u. To see how these work proceed as follows. For each x, $0 < x \leqslant a$, the quantity $N_u(x)$ is determined as described above, and since $N_u(x)$ is a simple step function in x its intervals of constancy can be displayed along the vertical axis. Consider those x-values, $x_1, \ldots, x_N$, say, at which $N_u(x)$ changes; in the two examples given $N = 4$. At these points calculate.

$$C_j = N_u(x_j) - N_u(x_j^-),$$

which could be called the jth contribution to φ. Since the limit defining C_j is one-sided, C_j will be zero for some values of j. Finally, $\varphi(A_u)$ is given by $\Sigma_j C_j$.

A heuristic understanding of the upcrossing characteristic can be gained by noting the following facts: if the excursion set A_u is composed of a single simply connected set without holes that does not intersect the boundary ∂S of S, then $\varphi(A_u) = 1$; if A_u is composed of k such sets then $\varphi(A_u) = k$; if k such components of A_u contain a total of m holes, then $\varphi(A_u) = k - m$; etc. If A_u does intersect ∂S, a 'boundary correction factor' amounting to the number of upcrossings of the processes $X(0, t)$, $0 \leqslant t \leqslant b$, and $X(s, 0)$, $0 \leqslant s \leqslant a$, plus one if $X(0, 0) \geqslant u$, has to be subtracted.

The upcrossing characteristic has many useful properties, all of which are enumerated in detail in Adler (1981). The property that is most relevant in the current setting, however, is that for both Gaussian and χ^2_n random surfaces its expected value can be written in a neat closed form. For a Gaussian surface $X(s, t)$ we have

$$\mathscr{E}\{\varphi[A_u(X, S)]\} = m(S)\,(2\pi)^{-\frac{3}{2}}\,\Lambda^{\frac{1}{2}}\sigma^{-3}u \exp\,(-u^2/2\sigma^2), \tag{3.8}$$

where $\Lambda = \lambda_{20}\lambda_{02} - \lambda_{11}^2$, and the λ_{ij} are given by (2.4). We denote the area of S by $m(S)$. For a χ^2_n-surface $Y(s, t)$, whose component fields $X_i(s, t)$ have variance σ^2 and second spectral moments λ_{ij}, we have

$$\mathscr{E}\{\varphi[A_u(Y, S)]\} = \frac{m(S)\,u^{\frac{1}{2}(n-2)}\,\Lambda^{\frac{1}{2}}}{2^{\frac{1}{2}n}\pi\sigma^n\,\Gamma(\frac{1}{2}n)}\left[\frac{u}{\sigma^2} - (n-1)\right]\exp\left(-\frac{u}{2\sigma^2}\right). \tag{3.9}$$

(Note that whereas in (3.8) u can take both negative and positive values, (3.9) is valid only for $u > 0$, since a χ^2_n-process is, by definition, always positive. Furthermore, (3.9) breaks down when $u = 0$ for technical reasons detailed in Adler (1981).

Although (3.9) is valid for χ^2_n-surfaces, $Y(s,t)$, and we shall be later working with M-inverted surfaces $Z(s,t) = M - Y(s,t)$, this result also provides the expected up-crossing characteristic for M-inverted surfaces. Noting that $A_u(Y,S) = [A_{M-u}(Z,S)]^c$, where B^c denotes the complement of B in S, and using the fact that $\varphi(B) = -\varphi(B^c)$ for every subset B of S, we obtain, for $u < M$,

$$\mathscr{E}\{\varphi[A_u(Z,S)]\} = \frac{-m(S)\,(M-u)^{\frac{1}{2}(n-2)}\Lambda^{\frac{1}{2}}}{2^{\frac{1}{2}n}\pi\sigma^n\,\Gamma(\frac{1}{2}n)}\left[\frac{(M-u)}{\sigma^2} - (n-1)\right]\exp\left[-(M-u)/2\sigma^2\right]. \quad (3.10)$$

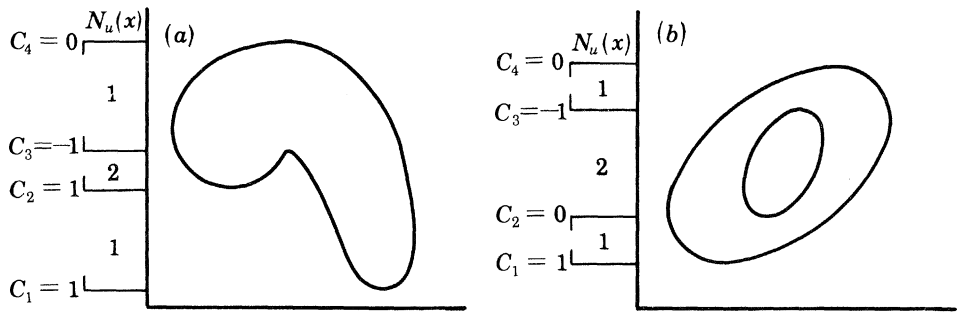

FIGURE 6. Computing the up-crossing characteristic: (*a*) $\varphi(A_\mu) = 1$; (*b*) $\varphi(A_\mu) = 0$.

This result, as well as the corresponding one for Gaussian surfaces, will, in the following section, form the basis for rejecting a rough surface model generated by 'transformation to normality' in favour of an M-inverted χ^2_n-model. Before we can do this, however, we have to allow for one more difficulty generated by the data.

The method described above for determining the upcrossing characteristic of a random surface implicitly assumed that the excursion sets, or, alternatively, the contour lines of the surface, were known. Of course this sort of information is often difficult to obtain, the data generally coming in the form of heights of the surface over some regular grid. This, for example, is so for the data described in § 3*a*. It is fortunate that, if the grid is fine enough, the upcrossing characteristic can be approximated by using only grid data.

To see how an approximation can be obtained, let L_n, $n \geqslant 1$, denote the lattice of points in the plane of the form $(i/n, j/n)$, i,j integers, and consider the example in figure 7, with a single closed curve enclosing the excursion set A_u. Also in this illustration is the grid L_8, a 'natural' approximation to A_u obtained by joining with horizontal or vertical lines all neighbouring points of L_8 lying in A_u. For general $n \geqslant 1$, let $N_n(\mathrm{S})$ denote the number of 'squares', i.e. quadruples of L_n-points, in the approximation to A_u based on L_n. Strictly $N_n(\mathrm{S})$ is also a function of u, but we can drop this parameter without causing confusion. Similarly, let $N_n(\mathrm{V})$, $N_n(\mathrm{H})$ and $N_n(\mathrm{P})$ denote, respectively, the number of vertical and horizontal lines (i.e. neighbouring pairs of L_n-points), and points of L_n in this approximation. Then note for the example of figure 7 we have $N_8(\mathrm{S}) = 3, N_8(\mathrm{V}) = 11, N_8(\mathrm{H}) = 9, N_8(\mathrm{P}) = 18$, and $N_8(\mathrm{S}) - [N_8(\mathrm{V}) + N_8(\mathrm{H})] + N_8(\mathrm{P}) = 1 = \varphi(\mathrm{A}_u)$. Relations of this form in fact hold in general, although we have to introduce a boundary correction term to cover the case when A_u intersects one or other of the axes. To this end let us write $N^*_n(\mathrm{V})$ and $N^*_n(\mathrm{H})$ to denote the number of pairs of neighbouring points of L_n both of which lie in A_u and are on the vertical and horizontal axes respectively. Similarly, let $N^*_n(\mathrm{P})$ denote the number

of points of L_n on either axis lying in A_u. Then we have the following result, which gives us the required approximation:

$$\varphi(A_u) = \lim_{n\to\infty} \varphi_n(A_u), \tag{3.11}$$

where

$$\varphi_n(A_u) = N_n(\mathrm{S}) - [N_n(\mathrm{V}) + N_n(\mathrm{H})] + N_n(\mathrm{P}) - [N_n^*(\mathrm{V}) + N_n^*(\mathrm{H})] + N_n^*(\mathrm{P}). \tag{3.12}$$

(For details on the type of convergence in (3.11) and a proof when the underlying random surface is Gaussian see Adler (1977, 1981). The proof for the χ_n^2-case is virtually identical to that in the Gaussian situation.)

The approximation given by (3.12) is particularly simple to apply, by computer, when the data are given in grid form.

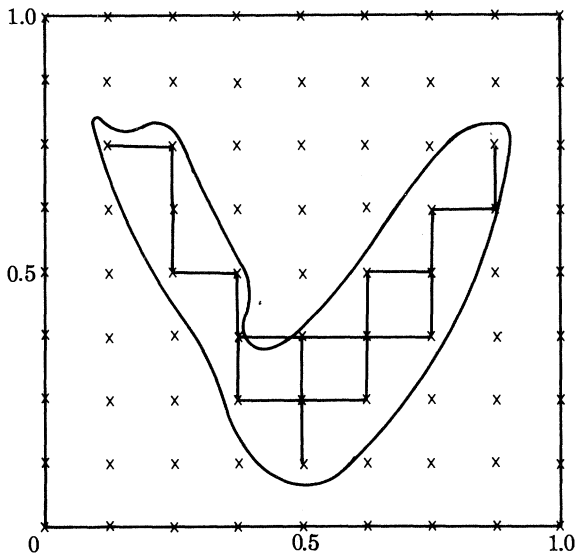

FIGURE 7. Obtaining the upcrossing characteristic by approximation on a square grid. The excursion set is contained within the unit square, and the points of the grid L_8 are marked with crosses.

Before concluding our discussion of upcrossing characteristics, it seems worth while to point out the connection between them and certain stereological concepts with which readers in materials science may be more familiar. The upcrossing characteristic is, in fact, little more than a generalization to excursion sets of the 'net tangent count' of DeHoff (1971), a concept that in one form or another seems to date back to at least the 1950s. Its introduction in Adler & Hasofer (1976) was motivated by a sterological study of Serra (1969). However, the upcrossing characteristic has a mathematical life of its own, as excursion sets, on which it is defined, do not generally satisfy the conditions required by stereologists for the sets that they study.

Another way to look at the upcrossing characteristic is to consider it as the Euler–Poincaré characteristic of the excursion set, with a boundary correction. (In fact, it was in this form that it was originally introduced.) Since the Euler–Poincaré characteristic is just one of a large class of Minkowski functionals (see, for example, Santalo (1976) for a discussion of these) one is immediately led to ask if other such functionals could also be used for surface fitting. The answer here must be negative, for no other functional yields such a neat, closed form for its expected value as does the Euler–Poincaré functional. (In fact, this closed form seems to arise more by

good luck than good management.) As an example, consider a close relative of the upcrossing characteristic, the 'absolute tangent count' of the excursion set, $\varphi_{\text{abs}}[A_u(X, S)]$, say, discussed in DeHoff (1978) and subsequently in Baddeley (1980). This is related to absolute curvature integrals and can be defined by altering (3.6) to

$$\varphi_{\text{abs}}[A_u(X, S)] = \sum_x |N_u(x) - N_u(x^-)|.$$

From § 5.4 of Adler (1981) we immediately obtain that if $X(s, t)$ is a Gaussian field then

$$\mathscr{E}\{\varphi_{\text{abs}}[A_u(X, S)]\} = m(S)\,(2\pi)^{-\frac{3}{2}}\,\Lambda^{\frac{1}{2}}\sigma^{-1}\exp\,(-u^2/2\sigma^2)$$
$$\times\left\{\frac{2u}{\sigma^2}\,\Phi\left[\frac{-\lambda_{11}u}{\sigma^2\nu_{11}-\lambda_{11}^2}\right]+\frac{2(\nu_{11}-\lambda_{11}^2/\sigma^2)}{(2\pi)^{\frac{1}{2}}\,\lambda_{11}}\exp\left[-\lambda_{11}^2u^2/2(\sigma^2\nu_{11}-\lambda_{11}^2)\right]\right\}$$

where Φ is the standard normal distribution function.

Not only is this formula far more complicated than that for the mean upcrossing characteristic, i.e. (3.8), but also it involves two more parameters, λ_{11} and ν_{11}. This is a substantial drawback in using this formula for surface fitting. Although an analogue of the above has never been derived for χ_n^2-surfaces, it is clear that, at the very least, it would involve the incomplete Γ-function, rendering it of little practical values. For, as we shall soon see, it is the simplicity of formulae (3.8)–(3.10) that makes them so useful in practice.

Finally, we note that the grid approximation outlined above also has its roots in the stereological literature (specifically Serra 1969) but, for technical reasons, needs to be rederived in the current setting.

(*d*) *An upcrossing analysis of the data*

We return now to the rough surface data of Bowyer described in § 3*a*. As figure 2 indicates, an appropriate model for these data would seem to be an M-inverted χ_n^2 random surface. In fitting such a model to the data, by estimating the parameters, M, n, and σ^2 of the model, we must proceed with some caution. The 15 000 observations that are summarized in the histogram of figure 2 are far from independent, and thus, as Switzer (1977) points out, analysing them as if they were independent could be highly misleading. In particular, the high positive correlation between close points on the surface would lead one to expect that the empirical histogram should exhibit less spread than exists in the true distribution, thus leading to an underestimate of the true population variance $2n\sigma^4$. Some bias is also to be expected.

To overcome this difficulty, on the one hand, and, on the other hand, to work with a method of estimation that places greater emphasis on the general structure of the surface than on its marginal distribution, we estimated the parameters of an M-inverted χ_n^2-model by fitting to the empirical upcrossing characteristics. In figure 8 the Bowyer upcrossing characteristics (obtained by using (3.12) with a grid size of 10 μm, so that $n = 100$) are displayed, for the levels $u = -22$ to $u = 10$. (The actual data, as figure 2 indicates, stop at about 9 μm. There were actually two grid points at which the surface height was above 9 μm. Here the heights were 17.58 μm and 11.34 μm. These two values have been replaced by values of 9.0 μm throughout the forthcoming analysis on the assumption that they either represent incorrect readings or, as isolated peaks, would be broken off as soon as the surface actually came in contact with another, thus making them irrelevant to the surface's gross behaviour.)

The solid line in figure 8 represents the expected upcrossing characteristic curve for an M-inverted χ_n^2-surface, calculated according to formula (3.10). The parameters M, n and σ^2

were chosen so as to obtain a best fit by a weighted least-squares criterion. The values of parameters so obtained were

$$M = 8.71, \quad n = 15, \quad \sigma^2 = 0.641, \quad \Lambda^{\frac{1}{2}} = 2553.8. \tag{3.13}$$

(The weights used were such as to yield a good fit in the right-hand half of the upcrossing curve, at the expense of the fit to the left-hand half. The rationale behind this lay in the fact that in practice only the surface peaks are of interest, and so it is the right-hand tails of the marginal distribution and upcrossing characteristic curve to which we want the best fit. In practice, the weighting seemed to have only little effect. For example, fitting by unweighted least squares yielded the estimates $M = 8.72$, $n = 16$, $\sigma^2 = 0.598$, $\Lambda^{\frac{1}{2}} = 2751.8$, and an expected upcrossing characteristic curve, that, on the scale of figure 8, was visually indistinguishable from the one given there.)

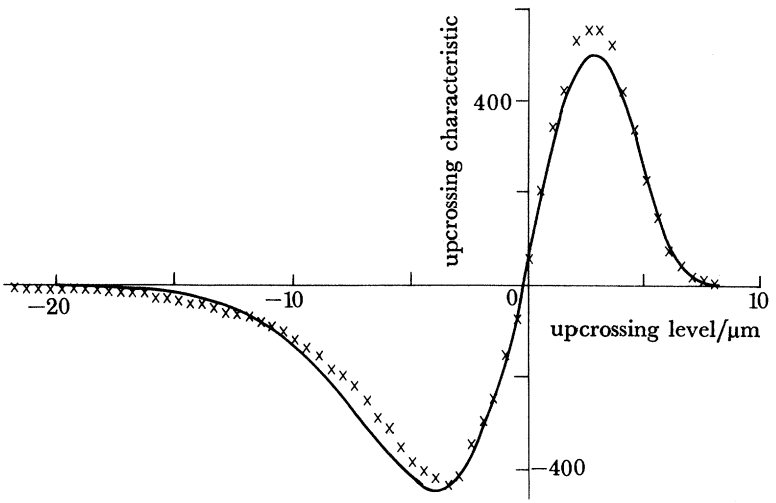

FIGURE 8. The upcrossing characteristics of the stainless steel data at various levels: ×, actual data; ——, least-squares fit obtained by using M-inverted χ_n^2-model.

Although the fit of the expected to the observed upcrossing rates in figure 8 seems most satisfactory, it is interesting at this stage to return to the marginal distribution of the surface to see how well a density function with parameters given by (3.13) fits the histogram of figure 2. This is shown in figure 9, where two fitted densities, one with $\sigma^2 = 0.641$, as in (3.13), and one with $\sigma^2 = 0.575$ are shown. It is clear that the density with the smaller variance gives a 'better' fit. However, in view of our previous comments, it is to be expected that the poorer fitting density, with parameters estimated from upcrossing characteristic curves, is actually the better estimate of the true density.

To examine whether an M-inverted χ_n^2-model is really needed, or whether a 'transformation to normality' of the type described in § 3 *b* suffices to place the data in the realm of a Gaussian model, the two transformations (3.1) and (3.2) were made. The transformed surfaces $Y_1(s, t)$ and $Y_2(s, t)$ each gave rise to their own observed upcrossing characteristic curves, to which were fitted expected curves on the basis of the Gaussian model (3.9). To enable fair comparison with the M-inverted χ_n^2-model, both the fitted and observed curves were transformed back to the original scale, and these are displayed in figure 10.

Although the fit for these transformed models is not totally unacceptable, it is certainly not as good as the fit depicted in figure 8. The residual sums of squares show this even more dramatically. A simple logarithmic transformation (3.1) yields a sum of squares of 493 847.9, while the more complicated model (3.2) yields 360 707.1. Both of these are an order of magnitude greater than that obtained with the M-inverted χ^2_n-model, where the (unweighted) residual sum of squares was 52 445.5. Thus we see that despite the fact that simple transformations made the normal probability plot look 'good', they did not yield surfaces whose upcrossing behaviour was consonant with that predicted by the Gaussian model.

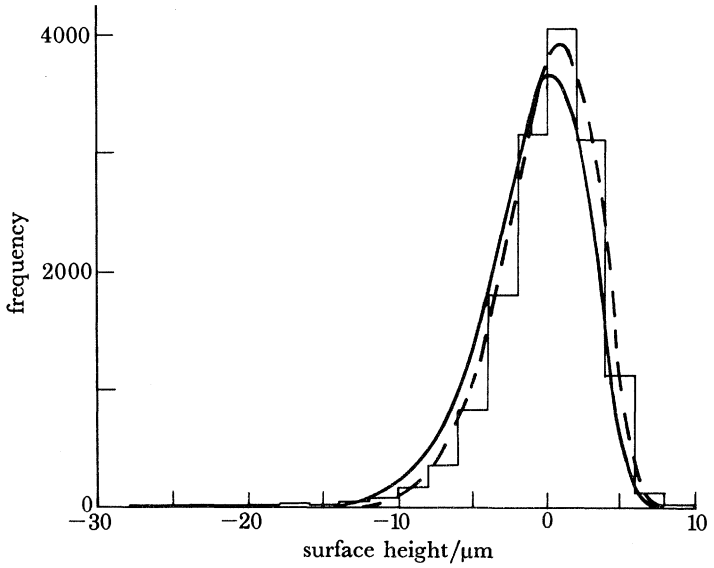

FIGURE 9. Histogram of surface heights of figure 2. The continuous curve is an M-inverted χ^2_n-model with parameter values (3.13). For the broken curve the parameter σ^2 has been reduced to 0.575.

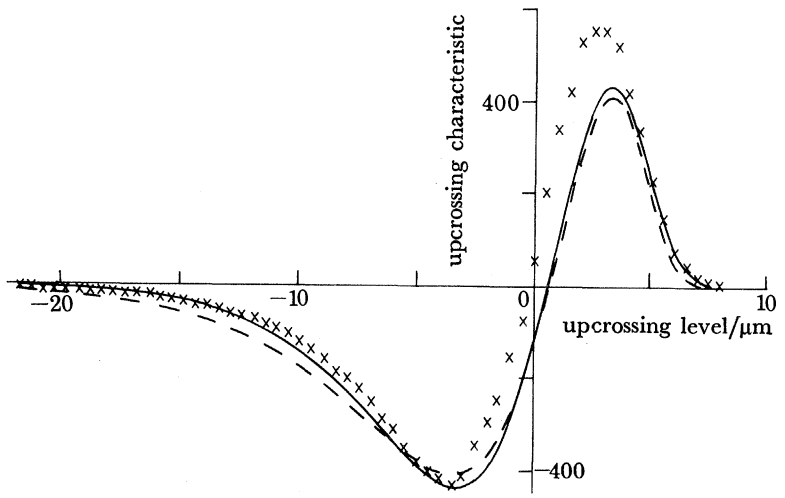

FIGURE 10. The upcrossing characteristics of the stainless steel data at various levels: ×, actual data; – – –, least-squares fit obtained by using the transformation (3.1) and the Gaussian model; ——, least-squares fit obtained by using the transformation (3.2) and the Gaussian model.

It is also important and interesting to note that using another transformation to normality that improves the fit of the transformed marginal distribution to a normal distribution cannot substantially improve the fit between the observed and fitted upcrossing characteristic rate. This is because any such transformation always leaves max (fitted rates) $= -$ min (fitted rates), a relation that the observed rates fail to satisfy.

Finally, we note for the interested reader that the techniques used in this section for parameter estimation and model identification are of significant independent interest, and are being further developed in a more complete statistical framework by Adler (in preparation).

We now leave the data-based justification of this new random surface model, and turn instead to an interesting theoretical point.

(*e*) *A theoretical consideration*

In the paper that introduced the Gaussian model of surface roughness, Greenwood & Williamson (1966) developed a simple mathematical model for the contact between a plane and a rough surface covered with a large number of asperities which, at least near their summits, are spherical. With no further assumptions other than that of a negative exponential distribution for the asperity heights, and that each asperity obeys the same area–compliance and load–compliance laws, their model exhibited exact proportionality between the expected values of the load and number of contact spots between the surfaces, and the conductance and area of contact. Having established that their microscopic model predicts these macroscopic phenomena, they proceed to state that '. . . although it will be shown later that height distributions tend to be Gaussian rather than exponential, the exponential distribution is nevertheless a fair approximation to the upper 25 % of the asperities of most surfaces.

We shall see later that the model proposed in this paper yields asperity distributions approximating negative exponential distributions in their tails even better than does a Gaussian model. Thus it seems that on the basis of the Greenwood & Williamson model of contact there are good theoretical grounds for accepting an M-inverted χ^2_n-model for surface roughness rather than the now almost classical Gaussian model.

4. Some preliminaries

In this section we begin our theoretical investigation of the model proposed in the preceding two sections by obtaining explicit expressions for certain multivariate probability densities that we shall require later. These are the density of the surface and its first- and second-order partial derivatives at a particular point, and a corresponding density for the surface *profile*, a concept that we shall define below.

Throughout the remainder of this paper we shall make the algebraically simplifying assumption that the component Gaussian surfaces $X_k(s,t)$ have been normalized, so that $\sigma^2 = 1$. Note that this implies that the variance of the χ^2_n- and M-inverted χ^2_n-surfaces $Y(s,t)$ and $Z(s,t)$ is $2n$, *not* 1, and that the scale change affected on $Y(s,t)$ and $Z(s,t)$ by dividing non-normalized $X_k(s,t)$ by σ is σ^2 rather than the more customary σ.

We begin with surfaces, and then consider profiles.

(*a*) *Surfaces*

In studying surfaces we shall need to make one more, rather restrictive, assumption, to reduce the complexity of the forthcoming algebra to manageable proportions. This assumption, which will be further discussed in § 7, is that $Y(s,t)$ is isotropic, i.e. its covariance function $R_Y(s,t)$ is a function of t^2+s^2 only. It follows immediately from (2.10) that $Y(s,t)$ will be isotropic if, and only if, the $X_k(s,t)$ are. The importance of this assumption is that it then follows from (2.5) (cf. Adler 1981, § 6.2) that the spectral moments λ_{ij} and ν_{ij} of § 2 are of the form

$$\left.\begin{aligned} \lambda_{02} = \lambda_{20} = \lambda, \qquad & \lambda_{11} = 0, \\ \nu_{04} = \nu_{40} = 3\nu_{22} = 3\alpha\lambda^2, \qquad & \nu_{31} = \nu_{13} = 0. \end{aligned}\right\} \tag{4.1}$$

for some $\lambda > 0$, where the parameter α is simply defined by

$$\alpha = \nu_{04}/\lambda^2. \tag{4.2}$$

Longuet-Higgins (1957*a*, p. 387) has shown that the parameter α lies in the range $(1.5, \infty)$, with increasing α corresponding to flatter spectra, and so to surfaces exhibiting roughness of shorter wavelength.

Let us now denote partial differentiation by superscripts, so that

$$\frac{\partial Y(s,t)}{\partial s} = Y^{(1)}(s,t), \quad \frac{\partial^2 Y(s,t)}{\partial s^i\, \partial t^j} = Y^{(i,j)}(s,t), \quad i+j = 2, \quad \text{etc.}$$

and let $\boldsymbol{Y}'$ and $\boldsymbol{Y}''$, respectively, be the vectors $(Y^{(1)}, Y^{(2)})$ and $(Y^{(2,0)}, Y^{(1,1)}, Y^{(0,2)})$.

The basic piece of information upon which most of the forthcoming analysis will rely is the joint probability density of $(Y, \boldsymbol{Y}', \boldsymbol{Y}'')$. We shall denote this by $f(y, \boldsymbol{y}', \boldsymbol{y}'')$. (In general, we shall henceforth use f as a generic expression for a probability density.) In particular, since we shall be primarily concerned with *critical* points of $Y(s,t)$, i.e. points (s,t) where $Y^{(1)}(s,t) = Y^{(2)}(s,t) = 0$ we require an expression for $f(y, \mathbf{0}, \boldsymbol{y}'')$. But this density can be factored as

$$f(y, \mathbf{0}, \boldsymbol{y}'') = f(\boldsymbol{y}''|y, \mathbf{0}) \quad f(y, \mathbf{0}), \tag{4.3}$$

and it turns out that the most convenient way to evaluate $f(y, \mathbf{0}, \boldsymbol{y}'')$ is to obtain each density in (4.3) independently. We commence with the conditional density.

From (2.7) we have that

$$Y^{(i,j)} = 2\sum_{k=1}^{n} X_k X_k^{(i,j)} + 2\sum_{k=1}^{n} X_k^{(i)} X_k^{(j)}, \quad i+j = 2. \tag{4.4}$$

Thus, if we condition on the event

$$\mathscr{A} = \{X_k = x_k, X_k^{(i)} = x_k^{(i)}, k = 1, \ldots, n, i = 1, 2\}$$

we immediately obtain that

$$\mathscr{E}[Y^{(i,j)}|\mathscr{A}] = 2\sum_{k=1}^{n} x_k \mathscr{E}[X_k^{(i,j)}|\mathscr{A}] + 2\sum_{k=1}^{n} [x_k^{(1)}]^i [x_k^{(2)}]^j.$$

But $\mathscr{E}[X_k^{(i,j)}|\mathscr{A}] = -x_k \lambda_{ij}$ (from (2.6) and the properties of multivariate normal distributions), so that

$$\mathscr{E}[Y^{(i,j)}|\mathscr{A}] = -2\lambda_{ij}\sum_{k=1}^{n} x_k^2 + 2\sum_{k=1}^{n} [x_k^{(1)}]^i [x_k^{(2)}]^j. \tag{4.5}$$

Similarly, (4.1), (4.2) and (4.4) give the conditional covariance matrix of Y'' as

$$4\sum_{k=1}^{n} x_k^2 \begin{bmatrix} \lambda^2(3\alpha-1) & 0 & \lambda^2(\alpha-1) \\ 0 & \alpha\lambda^2 & 0 \\ \lambda^2(\alpha-1) & 0 & \lambda^2(3\alpha-1) \end{bmatrix} = 4\sum_{k=1}^{n} x_k^2/\boldsymbol{M}, \quad \text{say.} \tag{4.6}$$

To convert to a more useful form of conditioning, we keep the X_k fixed and transform the $X_k^{(1)}$ and $X_k^{(2)}$ to variables V_k, W_k, where

$$V_1 = \sum_{k=1}^{n} x_k X_k^{(1)} \Big/ \Big(\sum_{k=1}^{n} x_k^2\Big)^{\frac{1}{2}}, \quad W_1 = \sum_{k=1}^{n} x_k X_k^{(2)} \Big/ \Big(\sum_{k=1}^{n} x_k^2\Big)^{\frac{1}{2}}, \tag{4.7}$$

and $V_2, \ldots, V_n$ and $W_2, \ldots, W_n$ are chosen so that the transformations $\{X_k^{(1)}\} \to \{V_k\}$ and $\{X_k^{(2)}\} \to \{W_k\}$ are identical and orthonormal. Then $V_1 = 0 \Leftrightarrow Y^{(1)} = 0$ and $W_1 = 0 \Leftrightarrow Y^{(2)} = 0$ (given $X_k = x_k$). Furthermore, the V_k and W_k have variance λ, and covariance 0, while the following identities hold:

$$\sum_{k=1}^{n} V_k^2 = \sum_{k=1}^{n} [X_k^{(1)}]^2, \quad \sum_{k=1}^{n} W_k^2 = \sum_{k=1}^{n} [X_k^{(2)}]^2, \quad \sum_{k=1}^{n} V_k W_k = \sum_{k=1}^{n} X_k^{(1)} X_k^{(2)}.$$

Thus we obtain from (4.5) and the above that, for example,

$$\mathscr{E}[Y^{(2,0)} | X_k = x_k, Y^{(1)} = Y^{(2)} = 0] = \mathscr{E}_{V_2, \ldots, V_n, W_2, \ldots, W_n}\Big(-2\lambda \sum_{k=1}^{n} x_k^2 + 2\sum_{k=2}^{n} V_k^2\Big)$$

$$= 2\lambda\Big[(n-1) - \sum_{k=1}^{n} x_k^2\Big].$$

In general, letting δ_{ij} denote the Kronecker delta, and $\delta_{ij}^* = 1 - \delta_{ij}$, we have

$$\mathscr{E}[Y^{(i,j)} | X_k = x_k, Y^{(1)} = Y^{(2)} = 0] = 2\lambda\delta_{ij}^*\Big[(n-1) - \sum_{k=1}^{n} x_k^2\Big].$$

It is now simple to convert to the conditioning $Y = y$ to obtain that, given $Y = y$, $Y^{(1)} = Y^{(2)} = 0$, the $Y^{(i,j)}$ have a multivariate normal distribution with means

$$\mathscr{E}[Y^{(i,j)} | Y = y, Y^{(1)} = Y^2 = 0] = 2\lambda\delta_{ij}^*(n-1-y), \tag{4.8}$$

and covariance matrix

$$4y\boldsymbol{M}, \tag{4.9}$$

where $\boldsymbol{M}$ is as in (4.6).

This suffices to establish the form of the conditional density in (4.3). We now turn our attention to the density for $(Y = y, Y' = \mathbf{0})$, i.e. $f(y, \mathbf{0})$. This, however, is considerably easier, and we use a technique of Hasofer (1970). Let $\boldsymbol{W}(s,t) = (W^{(1)}, W^{(2)})$ denote the vector variable $Y'(s,t)/[Y(s,t)]^{\frac{1}{2}}$ and $\mathscr{B}$ the event $\{X_k(s,t) = x_k, k = 1, \ldots, n\}$. Then, noting that the X_k are independent of one another, that from (4.1) and (2.6) $X_k^{(1)}$ is independent of $X_k^{(2)}$, and that both of these are independent of X_k, we immediately obtain that, conditional on $\mathscr{B}$, $W^{(i)}$ is given by

$$W^{(i)} = [x_i X_1^{(i)} + \ldots + x_n X_n^{(i)}]/(x_1^2 + \ldots + x_n^2)^{\frac{1}{2}}. \tag{4.10}$$

Thus the conditional distribution of $\boldsymbol{W}$ is bivariate normal with zero means, and covariance matrix $\lambda\boldsymbol{I}$, where $\boldsymbol{I}$ is the identity matrix. Since the distribution of $\boldsymbol{W}$ conditional on $\mathscr{B}$ is independent of the x_k, it follows that its unconditional distribution is normal and independent of the X_k. It is therefore independent of Y as well, and so the joint density of $\boldsymbol{W}$ and Y is given by

$$f(\boldsymbol{w}, y) = \frac{y^{\frac{1}{2}(n-2)} e^{-\frac{1}{2}y}}{2^{\frac{1}{2}n}\Gamma(\frac{1}{2}n)} \frac{1}{2\pi\lambda} \exp\left(-\{[w^{(1)}]^2 + [w^{(2)}]^2\}/2\lambda\right).$$

Making the transformation $(\boldsymbol{W}, Y) \to (\boldsymbol{Y}', Y)$ in the above, and setting $\boldsymbol{Y}' = \mathbf{0}$, immediately yields the required density

$$f(y, \mathbf{0}) = y^{\frac{1}{2}(n-4)} e^{-\frac{1}{2}y} / \lambda\pi 2^{\frac{1}{2}(n+6)} \Gamma(\tfrac{1}{2}n), \quad y \geqslant 0. \tag{4.11}$$

Combining this result with (4.8) and (4.9), via (4.3), yields $f(y, \mathbf{0}, \boldsymbol{y}'')$, which is the density we have been seeking.

(*b*) *Profiles*

In the following section we shall begin our investigation of the statistical properties of χ_n^2- and M-inverted χ_n^2-surfaces by considering initially corresponding properties of their *profiles*. These are the processes $Y(t)$ and $Z(t)$ obtained by restricting the surfaces $Y(x, y)$ and $Z(x, y)$ to straight lines of the form $x \sin\theta - y \cos\theta = C$. If the surfaces are homogeneous, then so are the profiles, and the covariance functions of the latter are simply determined by those of the former; for example

$$\begin{aligned} R_Y(t) &= \mathscr{E}[Y(s)\, Y(s+t)] \\ &= \mathscr{E}[Y(0,0)\, Y(t\cos\theta, t\sin\theta)] \\ &= R_Y(t\cos\theta, t\sin\theta). \end{aligned}$$

Similarly, the spectral moments of the profile processes are determined straightforwardly by those of the surfaces. Detailed formulae are given in Longuet-Higgins (1957*a*). Thus, in dealing with profiles, it is sufficient, and convenient, to treat them without reference to the underlying surface. Hence, throughout this and the following section, we shall assume that $Y(t)$ is an χ_n^2-process defined on the real line by

$$Y(t) = X_1^2(t) + \ldots + X_n^2(t), \tag{4.12}$$

where the $X_i(t)$ are independent, homogeneous Gaussian processes with zero mean and covariance function $R(t)$. Similarly, $Z(t) = M - Y(t)$ will denote an M-inverted χ_n^2-process. We shall denote the first three even-ordered spectral moments of $X_i(t)$ as follows:

$$\left.\begin{aligned} \sigma^2 = \mathscr{E}[X_i^2(t)] = R(0), \quad \lambda = \mathscr{E}\{[X_i'(t)]^2\} = -R''(0), \\ \nu = \mathscr{E}\{[X_i''(t)]^2\} = R^{(4)}(0). \end{aligned}\right\} \tag{4.13}$$

As in the study of surfaces, we shall again assume that $\sigma^2 = 1$. The implications of this assumption for profiles are identical to those for surfaces. We shall also introduce the parameter

$$\alpha = \nu/\lambda^2. \tag{4.14}$$

It is easy to check that $\alpha > 1$ for all processes in one dimension.

Again, for what follows, we shall require the joint probability density for (Y, Y', Y'') when $Y' = 0$. This can be obtained by using similar, but simpler, arguments to those used in studying surfaces, to yield that, conditionally on $(Y = y, Y' = 0)$, Y'' has a normal distribution with mean and variance respectively

$$2\lambda(n-1-y) \quad 4y\lambda^2(\alpha-1), \tag{4.15}$$

while the density for the conditioning event is given by

$$f(y, 0) = y^{\frac{1}{2}(n-3)} e^{-\frac{1}{2}y} / 2^{\frac{1}{2}(n+3)} \Gamma(\tfrac{1}{2}n)\, (\lambda\pi)^{\frac{1}{2}}. \tag{4.16}$$

(Compare (4.15) and (4.16) with (4.8), (4.9) and (4.11).)

Equations (4.15) and (4.16) immediately give

$$f(y,0,y'') = \frac{y^{\frac{1}{2}(n-4)}}{2^{\frac{1}{2}(n+4)}\Gamma(\frac{1}{2}n)\,\pi\lambda^{\frac{3}{2}}(\alpha-1)^{\frac{1}{2}}}\exp\left\{\frac{-1}{2(\alpha-1)}\left[y\alpha+\frac{(y''-\delta)^2}{4\lambda^2 y}+\frac{y''-\delta}{\lambda}\right]\right\}, \tag{4.17}$$

where
$$\delta = 2\lambda(n-1). \tag{4.18}$$

This is the required density.

Finally, we note that there are two reasons for studying profile processes. First, they are far from devoid of intrinsic interest, particularly as in many experimental situations profile data are all that is available. Secondly, their study serves as a comparatively simple introduction to the algebraically awkward manipulations required for the more involved study of surfaces.

5. Statistical properties of profiles

(a) *The mean number of maxima and minima*

For applications to the problems of rough surfaces, our central concern must lie with the behaviour of M-inverted χ^2_n-processes at their local maxima. However, we can, equivalently, concern ourselves with the local minima of χ^2_n-processes. To convert these results to the M-inverted case, we then need only substitute $\mathrm{M}-z$, $-z'$ and $-z''$ for y, y' and y'' in the final formulae. Since this is a notationally more convenient procedure, this is, in fact, what we shall do.

Let $\bar{M}(\underline{M})$ denote the expected number of maxima (minima) of a χ^2_n-process in unit time, and $\bar{C}$ the expected number of critical points, i.e. points at which $Y'(t) = 0$. Then

$$\bar{C} = \bar{M} + \underline{M}.$$

The mean number of minima per unit time is given by

$$\underline{M} = \int_{y=0}^{\infty}\int_{y''=0}^{\infty} |y''| f(y,0,y'')\,\mathrm{d}y'', \tag{5.1}$$

while $\bar{M}$ and $\bar{C}$ are given by the same expression with the inner integral converted to $-\infty < y'' < 0$ and $-\infty < y'' < \infty$ respectively. Compare with Cramér & Leadbetter (1967, p. 245), where (5.1) is developed for Gaussian processes. An identical argument suffices in the χ^2_n-case, under appropriate regularity conditions.)

To evaluate (5.1) explicitly we shall need to use the well known fact that if X is a normal random variable with mean and variance σ^2, then setting $X^+ = \max(0, X)$, we have

$$\mathscr{E}(X^+) = \mu[1-\Phi(-\mu/\sigma)] + [\sigma/(2\pi)^{\frac{1}{2}}]\exp(-\tfrac{1}{2}\mu^2/\sigma^2), \tag{5.2}$$

where
$$\Phi(u) = \frac{1}{(2\pi)^{\frac{1}{2}}}\int_{-\infty}^{u} \mathrm{e}^{-\frac{1}{2}u^2}\,\mathrm{d}u. \tag{5.3}$$

Applying this result, (4.17) and (4.18), and setting $u^* = n-1-u$ yield

$$M = \lambda^{\frac{1}{2}}\int_{u=0}^{\infty} p(u)\,\mathrm{d}u \tag{5.4}$$

where
$$p(u) = \frac{u^{\frac{1}{2}(n-3)}\mathrm{e}^{-\frac{1}{2}u}}{2^{\frac{1}{2}(n+3)}\Gamma(\frac{1}{2}n)\,\pi^{\frac{1}{2}}}\left\langle 2u^*\Phi\left\{\frac{u^*}{[u(\alpha-1)]^{\frac{1}{2}}}\right\}+\left[\frac{2u(\alpha-1)}{\pi}\right]^{\frac{1}{2}}\exp\left[\frac{-(u^*)^2}{2(\alpha-1)u}\right]\right\rangle. \tag{5.5}$$

Both $\bar{M}$ and $\bar{C}$ can be expressed as integrals of similar expressions. The integral in (5.4) can be simplified to yield the following:

$$M = \frac{\lambda^{\frac{1}{2}}(\alpha-1)^{\frac{1}{2}}}{2^{\frac{1}{2}n}\pi\,\Gamma(\tfrac{1}{2}n)}\,\mathrm{e}^{(n-1)/(\alpha-1)}\left[\frac{n-1}{\alpha^{\frac{1}{2}}}\right]^{\frac{1}{2}n} K_{\frac{1}{2}n}\left[\frac{(n-1)\,\alpha^{\frac{1}{2}}}{\alpha-1}\right] + \frac{\lambda^{\frac{1}{2}}}{2^{\frac{1}{2}n}\,\Gamma(\tfrac{1}{2}n)\,(2\pi)^{\frac{1}{2}}}\int_{u=0}^{\infty} u^{*}u^{\frac{1}{2}(n-3)}\,\mathrm{e}^{-\frac{1}{2}u}\,\Phi\left\{\frac{u^{*}}{[u(\alpha-1)]^{\frac{1}{2}}}\right\}du. \tag{5.6}$$

(Here we have used the fact that

$$\int_{u=0}^{\infty} u^{m-1}\,\mathrm{e}^{au-b/u}\,\mathrm{d}u = 2\left(\frac{b}{a}\right)^{\frac{1}{2}m} K_m[2(ab)^{\frac{1}{2}}], \tag{5.7}$$

$a, b > 0$, where $K_m(x)$ is a modified Bessel function of the second kind (Gradshteyn & Ryzhik 1965).)

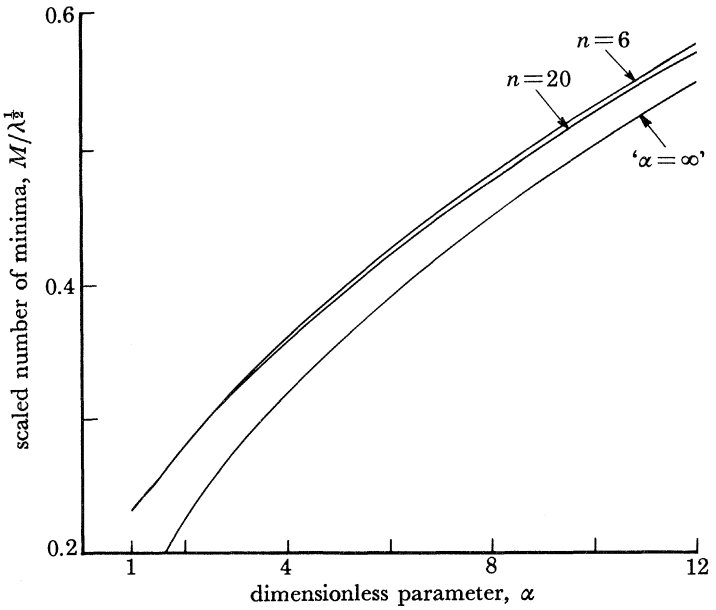

FIGURE 11. Scaled expected number of local minima of χ^2_n-profile per unit interval. The upper two curves are calculated from (5.6), while the lower curve is obtained from the asymptotic result (5.8).

To investigate (5.6) more closely, let $\alpha \to \infty$; i.e. let the spectra become flat. Then since

$$K_m(z) \sim \tfrac{1}{2}\Gamma(m)\,(\tfrac{1}{2}z)^{-m}$$

for small z, the first term on the right-hand side of (5.6) behaves like $(\lambda\alpha)^{\frac{1}{2}}/2\pi$ as $\alpha \to \infty$. The integral converges to zero as $\alpha \to \infty$. Thus

$$\underline{M} \sim (\lambda\alpha)^{\frac{1}{2}}/2\pi, \quad \text{large } \alpha. \tag{5.8}$$

This is an unexpected and surprising result, since, in the current parametrization, standard results (see, for example Cramér & Leadbetter 1967) give us that the mean number of local minima (or maxima) of each of the $X_k(t)$ processes is given by

$$\underline{M} = (\lambda\alpha)^{\frac{1}{2}}/2\pi \tag{5.9}$$

for all λ and α.

The (asymptotic) approximation given in (5.8) is actually remarkably good for virtually all values of n and α, as demonstrated in figure 11, where $\underline{M}/\lambda^{\frac{1}{2}}$ is plotted for various values of n and α.

Similar formulae can be developed for $\bar{M}$ and $\bar{C}$, all of which are readily amenable to numerical evaluation.

(*b*) *An aside on conditional probabilities*

In the following two subsections, and again in § 6, we wish to talk about probabilities such as 'the probability that $Y(0) \leqslant u$ *given that* $Y(t)$ *had a local minimum at* $t = 0$'. Since, in general, there will be zero probability of this event occurring at the instant $t = 0$, considerable care must be taken in defining such conditional probabilities. For this example we shall choose to define it as the ratio of the expected number of local minima in unit time at which $Y(t) \leqslant u$ to the expected number of local minima in unit time. Since standard extensions of (5.1) give this ratio as

$$\underline{M}^{-1} \int_{y=0}^{u} \int_{y''=0}^{\infty} |y''| f(y, 0, y'') \, \mathrm{d}y \, \mathrm{d}y'',$$

we can differentiate this expression with respect to u to obtain a conditional density for $Y(0)$ given by

$$\underline{M}^{-1} \int_{y''=0}^{\infty} |y''| f(u, 0, y'') \, \mathrm{d}y''. \tag{5.10}$$

We shall denote this by $f(u \| \text{local min})$, to differentiate between this type of conditioning (on process behaviour) and the simpler type of conditioning (on random variable behaviour) used, for example, in (4.3).

We shall in general approach conditional probabilities in this fashion. This choice of conditioning – by taking ratios of expectations – may be justified by noting that under appropriate regularity conditions (including ergodicity), this definition is equivalent to the so-called *horizontal window* conditioning of Kac & Slepian (1959). For further details regarding processes see Cramér & Leadbetter (1967), while for fields see Adler (1981), Wilson & Adler (1982), or Lindgren (1972).

(*c*) *The conditional density of heights at maxima and minima*

Suppose Y has a local minimum at the point $t = 0$. Then, according to the above, the conditional density for $Y(0)$ is given by (5.10). However, the integral in (5.10) is easy to evaluate, for we have,

$$f(u \| \text{min}) = \underline{M}^{-1} f(u, 0) \int_{y''=0}^{\infty} |y''| f(y'' | u, 0) \, \mathrm{d}y'',$$

where $f(u, 0)$ is given by (4.16). But, using the results of § 5 (*b*) we have that

$$f(u \| \text{min}) = p(u) \Big/ \int_0^{\infty} p(u) \, \mathrm{d}u, \tag{5.11}$$

where $p(u)$ is as given by (5.5). Note that the only parameters appearing in this density are α and n.

Examples of this density for various values of n, and α are given in figure 12. A feature common to all these examples is the significant skewness of the distribution, corroborating our contention in § 2*a* that any skewness in the profile distribution will also be exhibited in the distribution of extrema heights. In general, the conditional distribution is very similar to the unconditional distribution, shifted to the left. The similarity is a consequence of the fact that the minima are a sample, albeit non-random, from the unconditional distribution, while the shift is a consequence of the bias of the sampling.

PHILOSOPHICAL TRANSACTIONS OF THE ROYAL SOCIETY A MATHEMATICAL, PHYSICAL & ENGINEERING SCIENCES

It is possible to derive the conditional distribution of profile heights at local maxima of the χ^2_n-surface in precisely the same fashion as that for minima was obtained. This is given by

$$f(u\|\max) = g(u)/\bar{M}, \tag{5.12}$$

where $\bar{M} = \int_0^\infty g(u)\,du$ and

$$g(u) = \frac{\lambda^{\frac{1}{2}} u^{\frac{1}{2}(n-3)} e^{-\frac{1}{2}u}}{2^{\frac{1}{2}n}\Gamma(\frac{1}{2}n)\,(2\pi)^{\frac{1}{2}}} \left\langle u^* \Phi\left\{\frac{-u^*}{[u(\alpha-1)]^{\frac{1}{2}}}\right\} + \left[\frac{(\alpha-1)\,u}{2\pi}\right]^{\frac{1}{2}} \exp\left[\frac{-(u^*)^2}{2(\alpha-1)\,u}\right]\right\rangle.$$

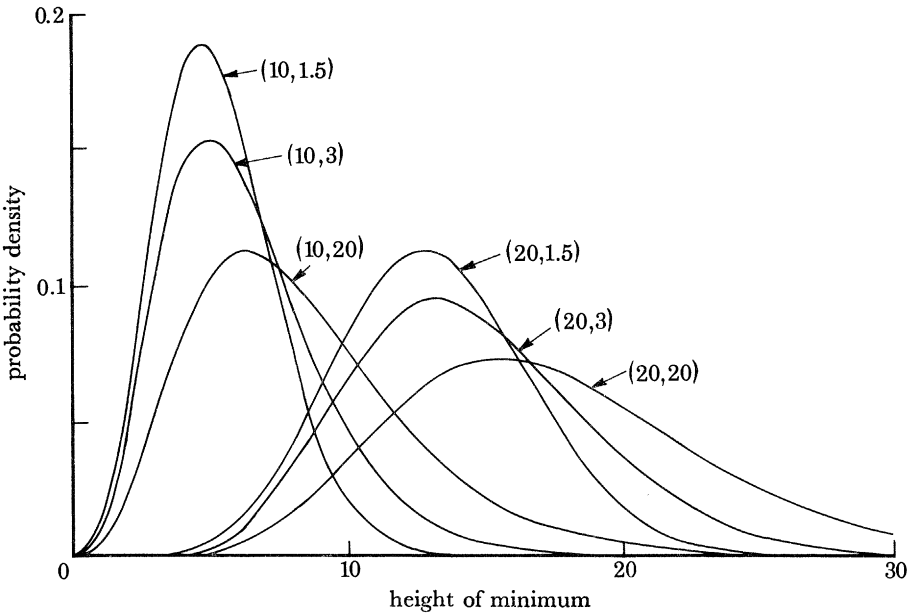

FIGURE 12. Probability density for heights of local minima of χ^2_n-profiles. The pair of numbers associated with each curve gives the values of the parameters n and α in that order.

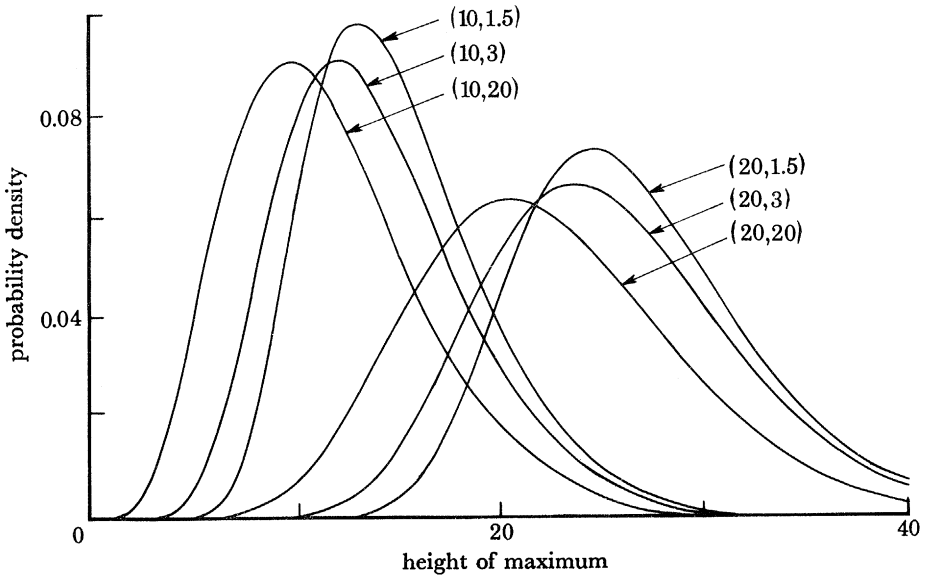

FIGURE 13. Probability density for heights of local maxima of χ^2_n-profiles.

Some examples of this density are given in figure 13. Again the density exhibits the skewness inherent in the unconditional height density. However, as opposed to what occurs when conditioning on minima, the densities exhibit a shift to the right of the original distribution.

(*d*) *The conditional density of the curvature at maxima and minima*

Now let us suppose that Y has a local minimum at $t = 0$, and we are interested in the distribution of the curvature at that minimum, i.e. the distribution of $Y''(t)$. According to the approach adopted in § 4*b*, this will be given by

$$f(z\|\min) = \underline{M}^{-1}\,|z| \int_0^\infty f(u, 0, z)\,\mathrm{d}u, \quad z \geqslant 0. \tag{5.13}$$

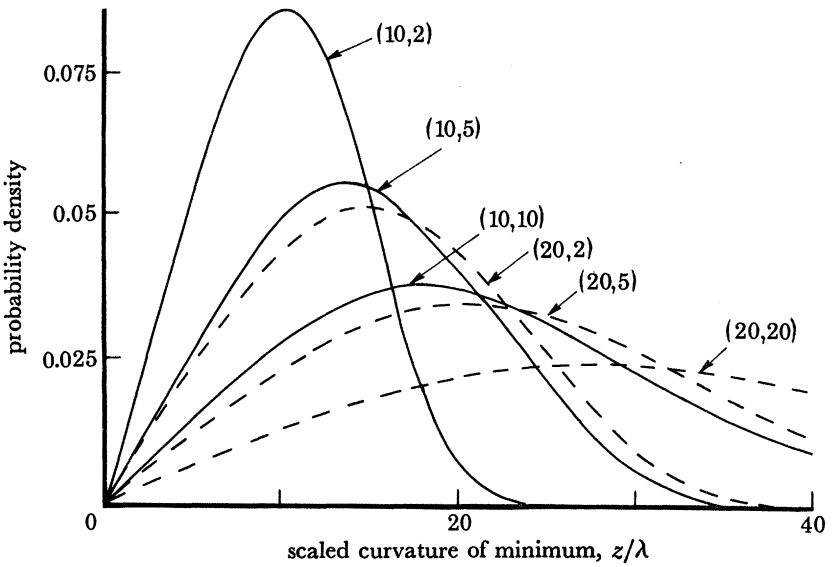

FIGURE 14. Probability density for scaled curvature of local minima of χ^2_n-profiles.

To evaluate the integral we again use the result (5.7), which together with (5.13) and (4.17) yields

$$\int_0^\infty f(u, 0, z)\,\mathrm{d}u = \frac{\mathrm{e}^{-(z-\delta)/2\lambda(\alpha-1)}\,|z-\delta|^{\frac{1}{2}(n-2)}}{2^n\Gamma(\frac{1}{2}n)\,\pi\lambda^{\frac{1}{2}(n+1)}\alpha^{\frac{1}{4}(n-2)}} K_{\frac{1}{2}(n-2)}\left[\frac{|z-\delta|\,\alpha^{\frac{1}{2}}}{2\lambda(\alpha-1)}\right].$$

To simplify this formula, we simply scale the curvature by λ^{-1}, to obtain from (5.13) and the above the scaled density

$$f(\lambda z\|\min) = \frac{2\lambda^{\frac{1}{2}}\,z|z-n+1|^{\frac{1}{2}(n-2)}\,\mathrm{e}^{-(z-n+1)/(\alpha-1)}}{\underline{M}\,2^{\frac{1}{2}n}\,\Gamma(\frac{1}{2}n)\,\pi\alpha^{\frac{1}{4}(n-2)}} K_{\frac{1}{2}(n-2)}\left[\frac{|z-n+1|\,\alpha^{\frac{1}{2}}}{2(\alpha-1)}\right]. \tag{5.14}$$

Note that since $\underline{M}$ is a multiple of $\lambda^{\frac{1}{2}}$ (cf. (5.6)), the right-hand side of the above equality is actually independent of λ. Examples of this density are given in figure 14.

Finally, we note that using the standard asymptotic expansion $(\pi/2z)^{\frac{1}{2}}\,\mathrm{e}^{-z}$ for $K_m(z)$ (see, for example, Abramowitz & Stegun 1965), we obtain from (5.13) and (5.14) that for large z

$$f(z\|\min) \sim C_n z(z-n+1)^{\frac{1}{2}(n-3)} \exp\{-(z-n+1)\,(1+\alpha^{\frac{1}{2}})/2\lambda(\alpha-1)\},$$

where C_n is the obvious normalization constant.

Using virtually identical arguments, the exact form and a similar asymptotic expansion can be developed for the density of the curvature at a maximum of the profile.

6. Statistical properties of surfaces

(a) *The mean number of maxima and minima*

As in § 5*a*, let $\underline{M}$ denote the mean number of local minima of $Y(s,t)$ as (s,t) ranges over the unit square. Then according to the corollary to theorem 5.1.1 of (Adler 1981), appropriate regularity conditions ensure that if $n > 1$

$$\underline{M} = \int_{u=0}^{\infty} \int_{A} |y^{(2,0)} y^{(0,2)} - [y^{(1,1)}]^2| f(u, \mathbf{0}, \mathbf{y}'') \, du \, d\mathbf{y}'', \tag{6.1}$$

where A is the set of $(y^{(2,0)}, y^{(1,1)}, y^{(0,2)})$ for which the matrix

$$\begin{bmatrix} y^{(2,0)} & y^{(1,1)} \\ y^{(1,1)} & y^{(0,2)} \end{bmatrix}$$

is positive definite. Writing (X, Y, Z) for $(Y^{(2,0)}, Y^{(1,1)}, Y^{(0,2)})$, (4.8) and (4.9) give us that the conditional probability density of these second-order partial derivatives can be written as

$$f(x,y,z|u,\mathbf{0}) = \frac{1}{(8\pi u)^{\frac{3}{2}} |\boldsymbol{M}|^{\frac{1}{2}}} \exp\left\{ -\frac{1}{8u} (x - 2\lambda u^*, y, z - 2\lambda u^*) \, \boldsymbol{M}^{-1} (x - 2\lambda u^*, y, z - 2\lambda u^*)' \right\}.$$

where
$$u^* = n - 1 - u, \quad |\boldsymbol{M}| = 4\alpha^2 \lambda^6 (2\alpha - 1), \tag{6.2}$$

and
$$\boldsymbol{M}^{-1} = \frac{1}{4\alpha^2\lambda^2(2\alpha-1)} = \begin{bmatrix} \alpha(3\alpha-1) & 0 & -\alpha(\alpha-1) \\ 0 & 4\alpha(2\alpha-1) & 0 \\ -\alpha(\alpha-1) & 0 & \alpha(3\alpha-1) \end{bmatrix}.$$

The exponent in the above can be expressed as follows:

$$-\frac{1}{8u}\{[\alpha(x+z) - 4\alpha\lambda u^*]^2 + y^2 4\alpha(2\alpha-1) + (x-z)^2 \alpha(2\alpha-1)\}/[4\alpha^2\lambda^2(2\alpha-1)].$$

Let us now make the substitution

$$t_1 = x + z, \quad t_2 = y_2, \quad t_3 = x - z.$$

Then note that
$$xz - y^2 = t_1^2 - t_2^2 - t_3^2,$$

while the condition that the matrix $\begin{bmatrix} x & y \\ y & z \end{bmatrix}$ is positive definite simplifies to $t_1^2 > t_2^2 + t_3^2$ and $t_1 > 0$. Noting that the Jacobian of this transformation is 2, we can substitute into (6.1) to obtain

$$\underline{M} = \frac{1}{16(2\pi)^{\frac{3}{2}} |\boldsymbol{M}|^{\frac{1}{2}}} \int_{u=0}^{\infty} u^{-\frac{3}{2}} f(u,0) \int_{t_1=0}^{\infty} \int\int_{t_2^2+t_3^2<t_1^2} (t_1^2 - t_2^2 - t_3^2) \times \exp\left[-\frac{1}{8u} \left| \frac{(t_1 - 4\lambda u^*)^2}{4\lambda^2(2\alpha-1)} + \frac{t_2^2}{\alpha\lambda^2} + \frac{t_3^2}{4\alpha\lambda^2} \right| \right] du \, dt_1 \, dt_2 \, dt_3. \tag{6.3}$$

Consider the inner triple integral, and convert to cylindrical coordinates, by setting

$$t_1 = z, \quad r = (t_2^2 + t_3^2)^{\frac{1}{2}}, \quad \theta = \arccos(t_2/r) = \arcsin(t_3/r).$$

Then the region of integration simplifies considerably to

$$0 < z < \infty, \quad 0 < r < z, \quad 0 < \theta < 2\pi,$$

while
$$t_1^2 - (t_2^2 + t_3^2) = z^2 - r^2.$$

Thus the inner integrals of (6.3) simplify to

$$\int_0^\infty \mathrm{d}z \int_0^{2\pi} \mathrm{d}\theta \int_0^z \mathrm{d}r (z^2 - r^2)\, r \exp\left[-\frac{r^2 h(\theta)}{32u\alpha\lambda^2} - \frac{(z - 4\lambda u^*)^2}{32u\lambda^2 (2\alpha - 1)} \right], \tag{6.4}$$

where

$$h(\theta) = 1 + 3\cos^2\theta. \tag{6.5}$$

Integrating out r simplifies (6.4) to

$$\int_0^\infty \mathrm{d}z \int_0^\pi \mathrm{d}\theta \exp\{-(z - 4\lambda u^*)^2 / 32u\lambda^2(2\alpha - 1)\} \times \left\{ \frac{2^4 u\alpha\lambda^2 z^2}{h(\theta)} - \frac{2^9 u^2\alpha^2\lambda^4}{h^2(\theta)} + \frac{2^9 u^2\alpha^2\lambda^4}{h^2(\theta)} \exp\left[-z^2 h(\theta) / 32u\alpha\lambda^2 \right] \right\}. \tag{6.6}$$

To integrate over z, we use the following result, easily established by integration by parts:

$$\frac{1}{(2\pi\sigma)^{\frac{1}{2}}} \int_0^\infty z^2 \mathrm{e}^{-\frac{1}{2}(z-\mu)^2/\sigma^2} \mathrm{d}z = (\sigma^2 + \mu^2)\, \Phi(\mu/\sigma) + \frac{\mu\sigma}{(2\pi)^{\frac{1}{2}}} \mathrm{e}^{-\frac{1}{2}\mu^2/\sigma^2}.$$

Tedious, but routine, integration then simplifies (6.6) to (6.8), in which

$$g^2(\alpha, \theta) = 1 + [(2\alpha - 1)/\alpha]\,(1 + 3\cos^2\theta), \tag{6.7}$$

$$2^{10} u^{\frac{5}{2}} \alpha\lambda^5 [2\pi(2\alpha - 1)]^{\frac{1}{2}} \int_0^\pi \mathrm{d}\theta \frac{1}{h(\theta)} \left\langle \left[(2\alpha - 1) + \frac{(u^*)^2}{u} \right] \Phi\left\{ \frac{u^*}{[u(2\alpha - 1)]^{\frac{1}{2}}} \right\} + \frac{u^*(2\alpha - 1)^{\frac{1}{2}}}{(2\pi u)^{\frac{1}{2}}} \exp\left[\frac{-(u^*)^2}{2u(2\alpha - 1)} \right] \right\rangle \frac{-2}{h^2(\theta)} \left\langle \Phi\left\{ \frac{u^*}{[u(2\alpha - 1)]^{\frac{1}{2}}} \right\} - \frac{1}{g(\alpha, \theta)} \Phi\left\{ \frac{u^*}{[u(2\alpha - 1)]^{\frac{1}{2}}} \right\} \exp\left\{ \frac{-(u^*)^2 [1 - g^{-2}(\alpha, \theta)]}{u(2\alpha - 1)} \right\} \right\rangle. \tag{6.8}$$

Integrating over θ, and substituting into (6.3), with the use of (6.2) and (4.11), finally yields

$$\underline{M} = \lambda \int_0^\infty p(u)\, \mathrm{d}u$$

where

$$p(u) = \frac{2u^{\frac{1}{2}(n-2)} \mathrm{e}^{-\frac{1}{2}u}}{\pi 2^{\frac{1}{2}n}\, \Gamma(\frac{1}{2}n)} \left\langle \left[(2\alpha - 1) + \frac{(u^*)^2}{u} - \tfrac{5}{4}\alpha \right] \Phi\left\{ \frac{u^*}{[u(2\alpha - 1)]^{\frac{1}{2}}} \right\} + \frac{u^*(2\alpha - 1)^{\frac{1}{2}}}{(2\pi u)^{\frac{1}{2}}} \exp\left\{ \frac{-(u^*)^2}{2u(2\alpha - 1)} \right\} + \frac{8\alpha}{\pi} \Phi\left\{ \frac{u^*}{[u(2\alpha - 1)]^{\frac{1}{2}}} \right\} \int_0^{\frac{1}{2}\pi} \frac{1}{h^2(\theta)\, g(\alpha, \theta)} \exp\left\{ \frac{-(u^*)^2 [1 - g^{-2}(\alpha, \theta)]}{u(2\alpha - 1)} \right\} \mathrm{d}\theta \right\rangle. \tag{6.9}$$

It is interesting, and useful, to note that as α becomes large both $p(u)$ and M simplify substantially. It is easy to check that for large α we have

$$p(u) \sim \frac{\alpha u^{\frac{1}{2}(n-2)} \mathrm{e}^{-\frac{1}{2}u}}{\pi 2^{\frac{1}{2}n}\, \Gamma(\frac{1}{2}n)} \left\{ \frac{3}{4} + \frac{8}{\pi 3^{\frac{1}{2}}} \int_0^{\frac{1}{2}\pi} [(1 + 3\cos^2\theta)^2 (1 + 2\cos^2\theta)^{\frac{1}{2}}]^{-1} \mathrm{d}\theta \right\} \approx 0.4408\, \alpha \frac{u^{\frac{1}{2}(n-2)} \mathrm{e}^{-\frac{1}{2}u}}{2^{\frac{1}{2}n}\, \Gamma(\frac{1}{2}n)}, \tag{6.10}$$

where the last approximation is obtained by numerical integration. Substitution into (6.8) and integration over u immediately yields that for large α

$$M \approx 0.4408\, \alpha\lambda. \tag{6.11}$$

Longuet-Higgins (1975*a*) showed that each of the component $X_k(s, t)$ fields has a mean number of local minima of

$$\alpha\lambda / 6\pi 3^{\frac{1}{2}} \approx 0.030\,63\, \alpha\lambda.$$

PHILOSOPHICAL TRANSACTIONS OF THE ROYAL SOCIETY A MATHEMATICAL, PHYSICAL & ENGINEERING SCIENCES

Thus we see that, quite unlike the situation with profiles, (cf. (5.8) and (5.9)) χ^2_n and Gaussian surfaces do not have similar numbers of local minima. We have not been able to find an intuitively appealing reason why this difference arises between one and two dimensions.

In figure 15 graphs of M/λ, as functions of α, are given for various values of n. As for profiles the convergence of the complicated formula (6.8) for M to the approximation based on (6.10) is gratifyingly rapid.

This completes our discussion of the mean number of local minima of a χ^2_n-process. As is the case with profiles, formulae similar to (6.8) and (6.9) could be developed for maxima and all critical points. However, we shall not do so here.

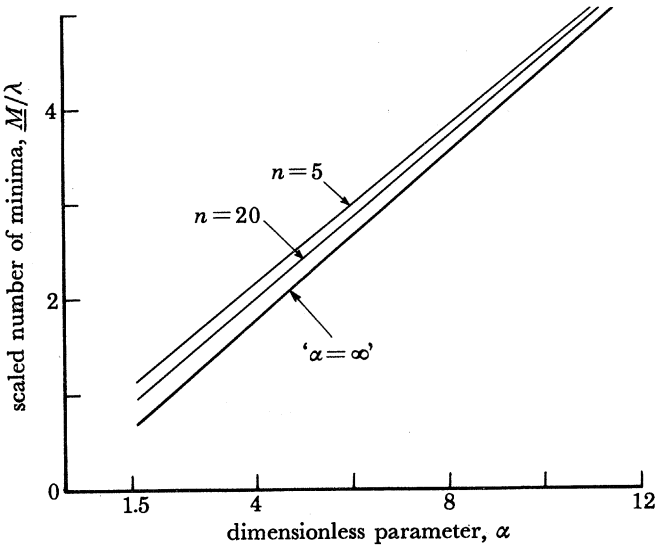

FIGURE 15. Scaled expected number of local minima of χ^2_n-surface per unit square. The upper two curves are calculated from (5.22) while the lower curve is obtained from the asymptotic result (5.24).

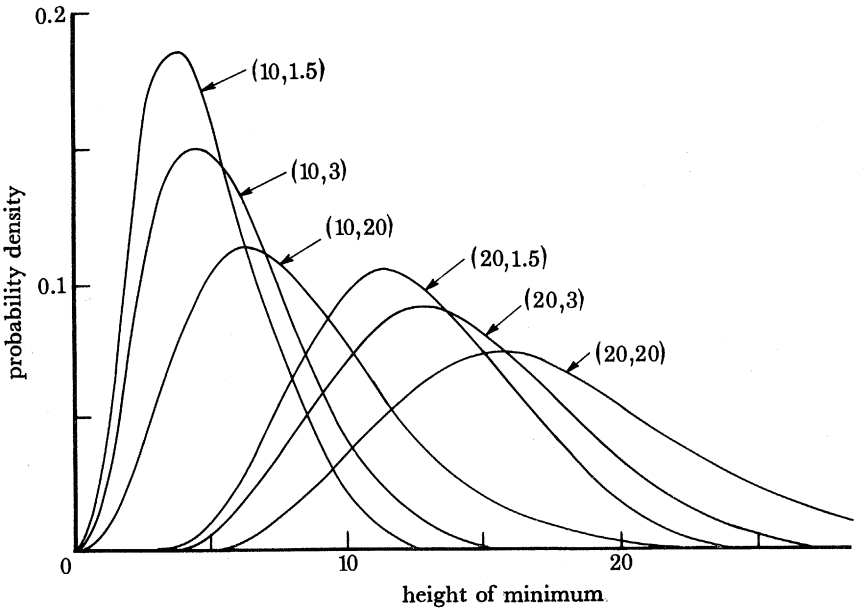

FIGURE 16. Probability density for heights of local minima of χ^2_n-surfaces.

(*b*) *The conditional density of heights at maxima and minima*

As we did when studying profiles, we shall again define conditional probabilities as ratios of expectations. Thus, if we condition on the event '$Y(s,t)$ has a local minimum at the point $s=t=0$' we automatically obtain the following conditional density for the height of this minimum:

$$f(u\|\min) = p(u)\Big/\int_0^\infty p(u)\,\mathrm{d}u, \tag{6.12}$$

where $p(u)$ is given by (6.9). Note that this density is parametrized by α and n only. Examples are given in figure 16, where, once again, the skewness of the underlying distribution is apparent.

Note that when α is large we obtain from (6.10) that

$$f(u\|\min) \approx u^{\frac{1}{2}(n-2)}\,\mathrm{e}^{-\frac{1}{2}u}/2^{\frac{1}{2}n}\,\Gamma(\tfrac{1}{2}n).$$

That is, the original χ^2_n-distribution is recovered.

(*c*) *The conditional density of the mean curvature at minima*

The mean curvature κ at any point on a surface is simply defined as the mean of the principle curvatures κ_1 and κ_2 at that point. However, as is noted by Nayak (1971), the sum of the curvatures along any two orthogonal directions at a point on the surface is equal to the sum of the principal curvatures. Thus the mean curvature at a minimum of $Y(s,t)$ is given by

$$\kappa = -\tfrac{1}{2}[Y^{2,0)}(s,t) + Y^{(0,2)}(s,t)]. \tag{6.13}$$

Our interest now lies in determining the distribution of κ at a minimum of $Y(s,t)$ at which $Y(s,t)=u$. With the same conditioning arguments as before, it follows from (6.6) by putting $\kappa = -\frac{1}{2}z$ that this density is given by

$$f(\kappa\|\text{min of height } u) = p(\kappa,u)\Big/\int_{-\infty}^0 p(\kappa,u)\,\mathrm{d}\kappa \tag{6.14}$$

where $u>0$, $\kappa<0$, and

$$p(\kappa,u) = \int_0^{2\pi}\mathrm{d}\theta\exp\left[-(\kappa-2\lambda u^*)^2/8u\lambda^2(2\alpha-1)\right]\left\langle\frac{u\kappa^2}{h(\theta)}-\frac{2u^2\alpha\lambda^2}{h^2(\theta)}\left\{1-\exp\left[\frac{-\kappa^2h(\theta)}{8u\alpha\lambda^2)}\right]\right\}\right\rangle. \tag{6.15}$$

If we now scale the mean curvature, setting $y=\kappa/\lambda\alpha^{\frac{1}{2}}=\kappa/\nu^{\frac{1}{2}}$, and integrate out θ where possible, we find we can replace (6.14) by

$$f(y\|\text{min of height } u) = g(y,u)\Big/\int_{-\infty}^0 g(y,u)\,\mathrm{d}y \tag{6.16}$$

where now $y<0$, $u>0$, and

$$g(y,u) = \exp\left[\frac{-(y-2u^*/\alpha^{\frac{1}{2}})^2}{8u(2-1/\alpha)}\right]\left\{y^2\pi u-5u^2+32u^2\int_0^{\frac{1}{2}\pi}h^{-2}(\theta)\exp\left[\frac{-y^2h(\theta)}{8u}\right]\mathrm{d}\theta\right\}. \tag{6.17}$$

Once again we have that the distribution of the normalized curvature at minima of specified heights, and so of any height, depends only on n and α.

An interesting, but unexpected, fact now arises from the above formulae. It is clear, from (6.15), that as $u\to 0$ the distribution of the non-normalized curvature tends to the distribution degenerate at $2\lambda(n-1)$.

PHILOSOPHICAL TRANSACTIONS OF THE ROYAL SOCIETY A MATHEMATICAL, PHYSICAL & ENGINEERING SCIENCES

This indicates the presence, in inverted χ^2_n-surfaces, of a phenomenon qualitatively and remarkably different to that present in the Gaussian model. At the high level maxima of a Gaussian surface the mean curvature is extremely large. In fact, it tends to infinity as the level tends to infinity. (Belyaev 1973; Nosko 1969). Thus high maxima tend to sit at the top of very sharp peaks. For M-inverted χ^2_n-surfaces, however, each maximum near the level M lies at the tip of a peak of almost fixed mean curvature, $2\lambda(n-1)$. This, presumably, is a consequence of the fact that M-inverted χ^2_n-surfaces are bounded above.

An important consequence of this phenomenon is that models of surface contact that assume a Gaussian model for the surface (see, for example, O'Callaghan & Cameron 1976, Nayak 1973*b*, Greenwood & Williamson 1966) can be expected to contain qualitative inaccuracies when the surface is better fitted by an inverted χ^2_n-model than a Gaussian one, as generally only the high level maxima are important in the modelling process. An indication of the type of inaccuracies that can arise, and how they can be resolved, is given in § 5 of Adler (1982).

7. Some further comments

In this, concluding, section we shall attempt to tidy up some of the loose ends left over from the preceding six sections.

The first comment we have to make relates to the problem of mathematical rigour. Throughout the paper we have always implicitly assumed that the various expectations we were taking were finite, and that the variables we were considering were well defined. However, this is, unfortunately, not always so. For example, if the component Gaussian surfaces $X_k(s,t)$ had exponential covariance functions of the form $R(s,t) = \exp(-\alpha s - \beta t)$, say, then they would have an infinite number of local maxima and minima, and all of our discussions about maxima and minima would be meaningless. In the main body of the paper we have neglected to make these implicit assumptions explicit, and moreover, have often done mathematical manipulations that are only valid under certain regularity conditions. These oversights were purposeful, as the paper was written to be read by practical people and not pure mathematicians. Nevertheless, it is important to note that regularity conditions are implicitly assumed throughout the entire paper. Details of these conditions in full generality are given in Adler 1981, ch. 7 and 3). A sufficient condition, however, for all of the results of this paper to be valid is that the covariance function $R(s,t)$ of the $X_k(s,t)$ satisfy the following inequality for all $i+j=4$, some $C>0$, and all (s,t) with s^2+t^2 small enough:

$$\left|\frac{\partial^4 R(s,t)}{\partial s^i\,\partial t^j} - \frac{\partial^4 R(0,0)}{\partial s^i\,\partial t^j}\right| \leqslant C(s^2+t^2). \tag{7.1}$$

In the Introduction we noted that the first serious attempt to build stochastic models of rough surfaces was via the three-point model of Greenwood & Williamson (1966). This model, while simple, was of considerable usefulness. Its mathematical simplicity lay in the fact that it was necessary to consider only three points on a profile at a given time, and thus one had only to deal with three-dimensional (Gaussian) distributions which, by virtue of a Markov property that was assumed to hold, simplified even further. In dealing with both χ^2_n-profiles, and (even Gaussian) surfaces, such mathematical simplification does not arise out of a three-point model. In the former case this is because trivariate (and even bivariate) χ^2_n-distributions are not as easy to manipulate as are their Gaussian counterparts. In the latter case, three points simply do not contain enough information about the local behaviour of a surface for any informative analysis to be undertaken. Consequently the type of model we have considered here is predicated not only

on the grounds that it is mathematically more sophisticated than a three-point type of model, but also on the grounds that the seemingly simpler model is, for profiles, not much simpler, and, for surfaces, uninformative.

In § 4 we imposed the restrictive assumption that the random surfaces we were considering were isotropic, which had the convenient effect of substantially simplifying the necessary mathematical manipulations. Unfortunately, not all real surfaces are isotropic. In fact, Bowyer's surface, which we explored in some detail in § 3, is distinctly anisotropic, as the surface exhibits quite distinct troughs and peaks parallel to the direction of grinding. This can be seen quite clearly in figure 17. Although one would expect that the qualitative aspects of the analysis of § 5 would be the same for isotropic and anisotropic surfaces, we have, at this stage, been unable to make a detailed analysis in the general situation. (Note, however, that the upcrossing characteristic analysis of § 3 does not assume isotropy.)

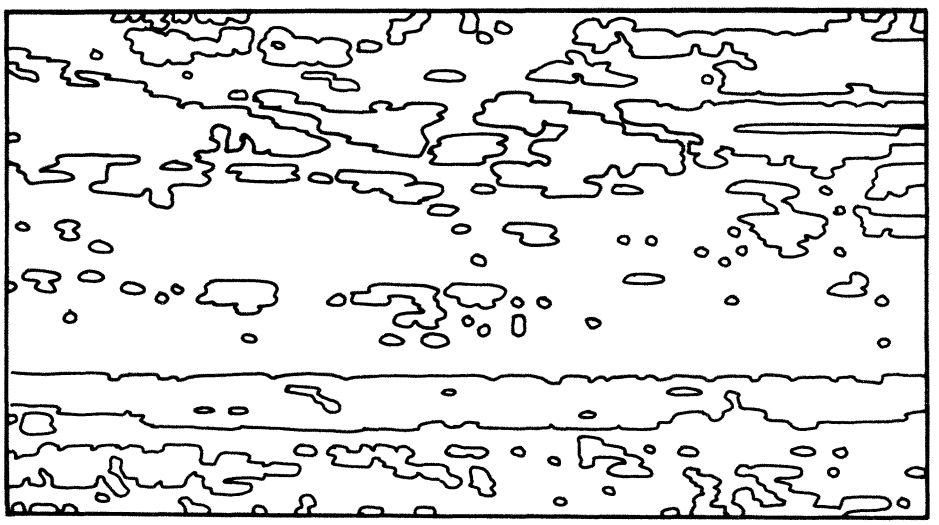

FIGURE 17. Contour lines at the level 2 μm of the stainless steel surface of Bowyer. The direction of grinding was parallel to the horizontal axis. The anisotropy of the surface is clear.

The final comment we have to make on the results of the preceding two sections is to note the fact, perhaps obvious, that we have not pushed the models to the limit in terms of obtaining densities for and expectations of every random variable of conceivable interest. For example, when dealing with surfaces in § 5*d* we considered the curvature at minima at a fixed level, while when dealing with profiles in § 4*e* we did not fix the level. However, we believe that we have presented enough detail for the interested reader to integrate over levels in § 5*d*, or to fix the level in § 4*e*, as well as to derive, without too great an effort, the distribution of virtually any other random variable (of a similar ilk to those already considered) that he may be interested in.

While doing the research reported in this paper, R. J. A. was supported in part by a Queen Elizabeth II Fellowship and in part by Technion VPR fund, grant number 190–527. D. F. was supported as a Professional Officer by the Australian Research Grants Council. We are grateful to all three bodies for their support.

A referee made an unusually careful reading of an earlier version of this paper, and suggested a number of changes which we feel have substantially improved its structure. We are also grateful to him.

PHILOSOPHICAL TRANSACTIONS OF THE ROYAL SOCIETY A MATHEMATICAL, PHYSICAL & ENGINEERING SCIENCES

References

Abramowitz, M. & Stegun, I. A. 1965 *Handbook of mathematical functions*. New York: Dover.

Adler, R. J. 1977 *Biometrika* **64**, 367–373.

Adler, R. J. 1981 *The geometry of random fields*. London: Wiley.

Adler, R. J. 1982 *Bull. int. statist. Inst.* **49** (To be published.)

Adler, R. J. & Hasofer, A. M. 1976 *Ann. Prob.* **4**, 1–12.

Archard, J. F., Hunt, R. T. & Onions, R. A. 1975 In *Proc. IUTAM Symposium on the Mechanics of Contact between Deformable Bodies* (ed. A. D. de Pater & J. J. Kalker), pp. 282–303. Delft University Press.

Baddeley, A. 1980 *Proc. Camb. phil. Soc.* **88**, 45–58.

Belyaev, Yu K. 1972 In *Proc. Sixth Berkeley Symp. Math. Statist. Prob.*, vol. 2, pp. 1–17. University of California Press.

Bowyer, A. 1980 Ph.D. thesis, University of London.

Bowyer, A. & Cameron, A. 1977 *Proc. Fourth Leeds–Lyon Symp.* London: Institute of Mechanical Engineers.

Cramér, H. & Leadbetter, M. R. 1967 *Stationary and related stochastic processes*. New York: Wiley.

Davenport, A. G. 1967 In *International Research Seminar on Wind Effects on Buildings and Structures*, pp. 19–82. Ottawa: University of Toronto Press.

De Hoff, R. T. 1971 *Trans metall. Soc. A.I.M.E.* **239**, 617–621.

De Hoff, R. T. 1978 In *Geometric probability and biological structures* (ed. R. E. Miles & J. Serra), *Lect. Notes Biomath.* **23**, 99–114.

Fuller, K. N. G. & Tabor, D. 1975 *Proc. R. Soc. Lond.* A **345**, 327–342.

Gradshteyn, I. S. & Ryzhik, I. M. 1965 *Table of integrals, series, and products*. New York: Academic Press.

Greenwood, J. A. & Williamson, J. B. P. 1966 *Proc. R. Soc. Lond.* A **295**, 300–319.

Hasofer, A. M. 1970 *Aust. J. Statist.* **12**, 150–151.

Hasofer, A. M. 1972*a* *Proc. Inst. civ. Engrs* **51**, 69–82.

Hasofer, A. M. 1972*b* *Proc. Inst. civ. Engrs* **53**, 599–605.

Hasofer, A. M. 1974 In *Studies in probability and statistics* (ed. E. J. Williams), pp. 153–159. Jerusalem: Academic Press.

Johnson, K. L. 1975 In *Proc. IUTAM Symposium on the Mechanics of Contact Between Deformable Bodies* (ed. A. D. de Pater & J. J. Kalker), pp. 26–40. Delft University Press.

Johnson, K. L., Kendall, K. & Roberts, A. D. 1971 *Proc. R. Soc. Lond.* A **324**, 301–313.

Kac, M. & Slepian, D. 1959 *Ann. math. Statist.* **30**, 1215.

Lindgren, G. 1972 *Ark. Mat.* **10**, 195–218.

Longuet-Higgins, M. S. 1957*a* *Phil. Trans. R. Soc. Lond.* A **249**, 321–387.

Longuet-Higgins, M. S. 1957*b* *Phil. Trans. R. Soc. Lond.* A **250**, 157–174.

Nayak, P. R. 1971 *Trans. Am. Soc. mech. Engrs, J. lubr. Technol.* **93**, 398–407.

Nayak, P. R. 1973*a* *Wear* **26**, 165–174.

Nayak, P. R. 1973*b* *Wear* **26**, 305–333.

Nosko, V. P. 1969 *Soviet Math.* **10**, 1481–1484.

O'Callaghan, M. & Cameron, M. A. 1976 *Wear* **36**, 79–97.

Onions, R. A. & Archard, J. F. 1973 *J. Phys.* D **6**, 289–304.

Santaló, L. A. 1976 *Integral geometry and geometric probability*, Addison–Wesley Encyclopaedia of mathematics series, vol. 1.

Serra, J. 1969 *Introduction à la morphologie mathématique, Cahiers du centre de morphologie mathématique* vol. 3. Paris: Ecoles de Mines.

Sharpe, K. 1978 *Adv. appl. Prob.* **10**, 373–391.

Silverman, B. 1980 In *Asymptotic theory of statistical tests* (ed. I. M. Chakravarti). London, New York: Academic Press.

Switzer, P. 1977 *Bull. int. statist. Inst.* **47**, 123–137.

Whitehouse, D. J. & Archard, J. F. 1970 *Proc. R. Soc. Lond.* A **316**, 97–121.

Wilson, R. G. & Adler, R. J. 1982 *Adv. appl. Probab.* **14** (in the press).

PHILOSOPHICAL TRANSACTIONS OF THE ROYAL SOCIETY A MATHEMATICAL, PHYSICAL & ENGINEERING SCIENCES